Measurement and Thermodynamic Modeling of Partition Coefficients in N,N-Dimethylacetamide – Water – Carbon Dioxide System

by

Nil Ezgi Dinçer

A Thesis Submitted to the
Graduate School of Engineering
in Partial Fulfillment of the Requirements for
the Degree of

Master of Science
in
Chemical and Biological Engineering

Koç University
August 2010

Koç University

Graduate School of Sciences and Engineering

This is to certify that I have examined this copy of a master's thesis by

Nil Ezgi Dinçer

and have found that it is complete and satisfactory in all respects,
and that any and all revisions required by the final
examining committee have been made.

Committee Members:

_____

Can Erkey, Ph. D. (Advisor)

_____

Seda Keskin, Ph. D.

_____

Erdem Alaca, Ph. D.

Date: 05.08.2010

To my family…

ABSTRACT

The partition coefficients of N,N-Dimethylacetamide (N,N-DMA) between the water and the supercritical carbon dioxide ($scCO_2$) phases were measured in the temperature range of 298.15 K – 318.15 K and the pressure range of 8.3 – 24.1 MPa. The measurements were carried out in a 56 ml vessel by contacting the supercritical and the aqueous phases. The partition coefficients of N,N-DMA were found to increase from 0.05 to 0.150 with increasing pressure at a constant temperature and increase with temperature at a constant density.

The bubble point pressures of N,N-DMA – CO_2 mixtures were measured at 298.15 K, 308.15 K and 318.15 K and were found to increase with increasing mole fraction of CO_2. The partition coefficients were modeled using the Peng-Robinson Equation of State (PREOS) combined with modified van der Waals mixing rule – The Panagiotopoulos and Reid mixing rule. The binary interaction parameters for the CO_2 – H_2O pair were taken from the literature and were regressed for CO_2 – N,N-DMA and H_2O – N,N-DMA pairs by fitting partition coefficients data. The binary interaction parameter for CO_2 – N,N-DMA pair was found to depend linearly on temperature. The bubble point pressures of N,N-DMA and CO_2 could be predicted fairly well using the regressed binary interaction parameters.

ÖZET

N,N-Dimetilasetamid (N,N-DMA)' in su ve süper kritik karbondioksit (skCO_2) fazı arasındaki dağılım katsayıları 298.15 K – 318.15 K sıcaklık değerleri arasında ve 8.3 – 24.1 MPa basınç değerleri arasında ölçülmüştür. Bu ölçümler 56 ml hacmindeki yüksek basınca dayanıklı paslanmaz çelik kapta süper kritik ve su fazı kontakt halinde olacak şekilde yapılmıştır. N,N-DMA' in dağılım katsayılarının 0.05' ten 0.150' ye sabit sıcaklıkta artan basınçla arttığı ve sabit yoğunlukta artan sıcaklık ile arttığı bulunmuştur.

N,N-DMA – CO_2 karışımının kabarcık noktası basınçları 298.15 K, 308.15 K ve 318.15 K' de ölçülmüştür ve CO_2' in artan mol kesri ile arttığı belirlenmiştir. Dağılım katsayıları Peng-Robinson Hal denklemi (PREOS) ile modifiye edilmiş van der Waals karışım kuralı - Panagiotopoulos ve Reid karışım kuralı kullanılarak modellenmiştir. CO_2 – H_2O çifti için ikili etkileşim parametreleri literatürden alınmıştır. CO_2 – N,N-DMA and H_2O – N,N-DMA çiftleri için ikili etkileşim parametreleri ise dağılım katsayı verilerine uyacak şekilde hesaplanmıştır. CO_2 – N,N-DMA çiftinin ikili etkileşim parametrelerinin sıcaklıkla doğrusal olarak değiştiği bulunmuştur. N,N-DMA ve CO_2 sisteminin kabarcık noktası basınçları bulunan etkileşim parametreleri kullanılarak uygun şekilde bulunmuştur.

ACKNOWLEDGEMENTS

I would like to thank my advisor Professor Can Erkey for his guidance and great support through my thesis project and graduate study, with his great knowledge and experience. He was not only my thesis advisor but also my guide who had influenced my future in career life. He gave me the chance and the support to gain important experience in academic life, take responsibility, participate in both international and national conferences and workshops, and write a journal article. Thanks to him, our research group had a lovely dinner meetings at beautiful places for special days. It was a pleasure to make research and study in his laboratory and learn lots of things from him. He will be a role model for me with his diligence, kindness, honesty and friendly attitude towards his students.

I am also grateful to Professor Seda Keskin and Professor Erdem Alaca for their support in my thesis work.

I would also like to thank Professor Halil Kavaklı and his research students Bengisu Seferoğlu and Onur Dağlıyan for their support in UV / VIS analysis.

Then, I thank to my colleagues Seda Giray, Selmi Bozbağ, Erdal Uzunlar, Deniz Şanlı, Zeynep Ülker and Oğuz Canıaz and also thank to former colleagues Seda Yaşar and Meriç Kartal for their help and support in the research laboratory during my graduate study. I also want to give my thanks to all of my friends at Koç University who made these two years an enjoyable period of time.

I would like to give my special and lots of thanks to Zeynep Kayserili, Murat Özsezer, Gökhan Dağlıoğlu and Melih Gürmeriç for being best friends of my life. They

were always like a family for me with their kindness, friendship and supports to make very important decisions. Most of my hard times would be unbearable without them and they made my life enjoyable.

Special thanks to the source of happiness and evenness, the reason of my life, the solution of every difficulty… My parents, Zehra and Murat Dinçer, my brother, Sezgi and my sister in law, Elvin, thanks are not enough to explain my gratitude to them for their great love, affection and friendship. They always supported me throughout my whole life. I love you so much.

TABLE OF CONTENTS

LIST OF TABLES

LIST OF FIGURES

NOMENCLATURE

Symbols

A	Constant
a	Attractive interaction parameter, cubic equations of state
a_i	Activity of component *i*
B	Constant
b	Covolume parameter, cubic equations of state
C	Parameter, Redlich – Kister equation
F	Number of intensive degrees of freedom
f_i	Fugacity of pure *i*
$\hat{f}_i$	Fugacity of component *i* in a mixture
G^E	Excess Gibbs Energy
K_x	Partition coefficient
K_{ij}	Binary parameter for interactions between species *i* and *j*
k_{ij}	Binary parameter for interactions between species *i* and *j*
N	Number of moles or molecules
n	Number of components
n_i	Number of moles component *i*
P	Absolute Pressure
P_c	Critical pressure
P_i	Partial pressure of mixture component *i*
Q	Heat flow
R	Gas law constant

T	Absolute temperature
T_c	Critical temperature
T_r	Reduced temperature
V	Specific volume
υ	Molar volume
x_i	Liquid mole fraction of component *i*
y_i	Vapor mole fraction of component *i*
Z	Compressibility factor

Greek Symbols

α	Function, cubic equations of state
γ_i	Activity coefficient of component *i*
k	Characteristic constant
κ	Characteristic constant
$\lambda_i(T)$	Temperature dependent term
μ_i	Chemical potential of component *i*
π	Number of phases
ρ	Density
ρ_r	Reduced density
$\hat{\phi}_i$	Fugacity coefficient of component *i* in a mixture
ω	Acentric factor

Chapter 1

INTRODUCTION

Removal of organic compounds from aqueous solutions is generally carried out using distillation which is a very energy intensive process or solvent extraction which requires the use of large quantities of hazardous and toxic organic solvents. An alternative technology which may be less energy intensive and environmentally friendly is supercritical fluid extraction. The lower viscosity and higher diffusivity of supercritical fluids than liquids may also lead to enhanced mass transfer rates. Among the supercritical fluids, supercritical carbon dioxide ($scCO_2$) is particularly attractive since it is non-toxic, environmentally friendly, non-flammable and relatively inert. As a result of these favourable properties as a solvent, extensive research has been carried out in laboratories around the world on supercritical extraction of a wide variety of organics such as alcohols, organic acids, ketones and polychlorinated biphenyls from water [1,2,3,4,5].

N,N-Dimethylacetamide (N,N-DMA) is a commodity chemical which is used in large quantities in many industries. Its high solubility in water and its excellent solvent power for high molecular weight polymers and resins make N,N-DMA a desirable solvent in fibre and polyurethane production. It is also a good reaction medium for the production of pharmaceuticals and cosmetics. Generally, it is mixed with water at some point along these processes. The resulting aqueous solutions are usually separated by a very energy intensive distillation process due to the high boiling point of N,N-DMA. The small impurities in these mixtures also lead to additional problems in distillation. Therefore, a process based on extraction of N,N-DMA from water using $scCO_2$ may be an attractive alternative to distillation.

The most important parameter which governs the economical feasibility of a $scCO_2$ extraction process for removal of an organic compound from water is the partition coefficient which is a measure of the distribution of the organic compound between the $scCO_2$ and aqueous phases. Therefore, we measured the partition coefficients of N,N-DMA between water and carbon dioxide phases in the temperature range of 298.15 K – 328.15 K and the pressure range of 80 – 240 atm. Thermodynamic models to predict the partition coefficients are important for extrapolation of data and in determination of optimum operation conditions. There have been two main approaches in the literature to model and predict the partition coefficients in organic-water-$scCO_2$ systems. One of these is to estimate the partition coefficients using linear solvation energy relationships (LSER) based on molecular structure [6]. This approach was used by Timko et al. to estimate the partition coefficients of 18 compounds including aldehydes, ketones, esters and halides between water and $scCO_2$ at 300 K and 80 bars. The second approach has been to use Equation of State (EOS) based methods. This approach has been used to model the partition coefficients of 2,4-dichlorophenol [2], phenol [7],benzene, naphthalene and parathion [8],p-chlorophenol, and m-cresol [9] and furfural [10] between water and supercritical carbon dioxide phases. In these studies, the fugacity coefficients for both supercritical and aqueous phases were calculated using the Peng Robinson EOS. In this study, we modeled the partition coefficients of N,N-DMA using fugacity coefficients for the supercritical phase and activity coefficients for the liquid phase. In addition, we studied the phase behaviour of N,N-DMA-CO_2 system by determining the bubble point pressures at 298.15, 308.15 and 318.15 K.

Chapter 2

LITERATURE REVIEW

2.1 Phase Equilibria and Partition Coefficients of Organic Substances in Water and Supercritical Carbon Dioxide ($scCO_2$)

2.1.1 Supercritical Fluids

A fluid is defined as a supercritical fluid (SCF) when it has been heated and compressed above its critical temperature and critical pressure. Above the critical temperature (T_c) and pressure (P_c) of a pure substance, phase separation does not occur. This means the critical point of a substance can be defined as the highest temperature and pressure at which gas and liquid phase can exist at the same time in equilibrium [11].

The pressure temperature diagram of a pure substance and schematic representation of arrangements of molecules in different states are shown in Figure 2.1. Along the solid lines in this figure, two different phases are in equilibrium and in the triple point three different phases coexist. In the supercritical region there is only a single homogenous phase when there are two phases in equilibrium in the phase boundaries. Therefore, it is possible for a substance to cross from a liquid state to gas state without any phase transition by passing through the supercritical region [12].

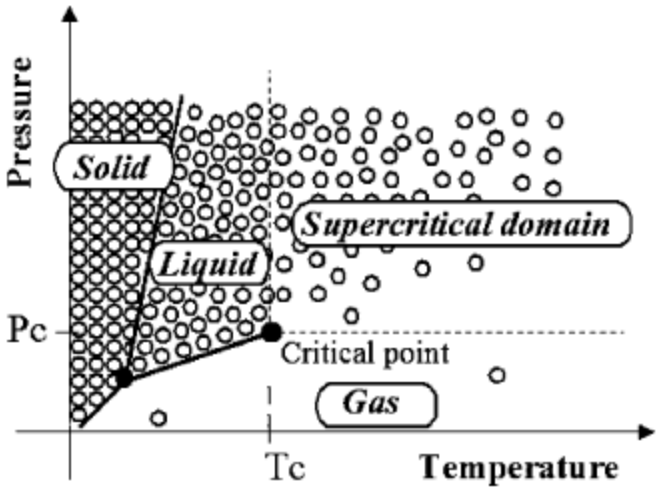

Figure 2.1 States of pure substance in the pressure – temperature diagram [12]

A comparison of the physical properties of common supercritical fluids with those of liquids and gases are given in Table 2.1. In the state of SCF, substance display properties which are intermediate to those of liquids and gaseous states. SCFs have greater densities than those of gases however comparable to those of liquids as shown in Table 2.1. This situation makes SCFs being used as solvents. SCFs have low viscosity combined with zero surface tension and the solutes have high diffusivity in SCFs therefore significant density gradients occur across the interface and provide easier mass transfer characteristics which leads to their development on an industrial scale for extraction process [12,13,14].

Table 2.1 Orders of Magnitude of Physical Properties of Solvents in Different States [14]

Property	Density, ρ (g/cm^3)	Diffusivity, D (cm^2/s)	Viscosity, η (g/cm·s)
Gas	10^{-3}	10^{-1}	10^{-4}
SCF	0.3 – 0.8	10^{-3}	10^{-4}
Liquid	1	$5x10^{-6}$	10^{-2}

Klesper, 1980

As the critical point of a compound is approached, its density changes dramatically because of the tendency of its isothermal compressibility to infinity. The density of substance can be adjusted with small variations of temperature and pressure in the critical region and this provides to regulate the solvent power of the supercritical fluid. The critical temperatures and pressures of some substances are shown in Table 2.2. These values of gases and liquids can be very different and thus specific supercritical fluids can be used for specific purposes. SCFs are preferential with their transport properties compared to conventional solvents. Supercritical fluids which have low critical temperature such as carbon dioxide are used as solvents for applications on heat-sensitive substances. On the other hand most industrial chemicals which are less temperature-sensitive can be processed with C_3 and C_4 hydrocarbons that have higher critical temperature [4,13].

Table 2.2 Critical Conditions of Pure Compounds [4]

Solvents	Critical Temperature (°C)	Critical Pressure (bar)
Carbon dioxide	31.1	73.8
Ethane	32.2	48.8
Ethylene	9.3	50.4
Propane	96.7	42.5
Propylene	91.9	46.2
Cyclohexane	280.3	40.7
Isopropanol	235.2	47.6
Benzene	289.0	48.9
Toluene	318.6	41.1
p-Xylene	343.1	35.2
Chlorotrifluoromethane	28.9	39.2
Trichlorofluoromethane	198.1	44.1
Ammonia	132.5	112.8
Water	374.2	220.5

The use of CO_2 as a solvent or raw material has been investigated somewhat continuously in academic research and/or industry since 1950. Interest in the use of CO_2 with these purposes has increased during the past 20 years as large – scale plants using CO_2 have been brought on line [15]. While supercritical fluids in general exhibit interesting physical properties [4], supercritical carbon dioxide (SC-CO_2) has a great potential for being preferred as a “green” solvent because it is nonflammable, relatively nontoxic, environment friendly, relatively inert. In addition, unlike water, CO_2 has low

critical temperature of only 31.1°C and moderate critical pressure of 73.8 bar [13,15,16]. These properties make SC-CO_2 one of the most beneficial and environmentally acceptable solvents used in manufacturing processes today.

2.1.2. Properties and Applications of N,N-Dimethylacetamide

N-Methylated acetamides are polar liquids that have high boiling points and very good solvency for both organic compounds and inorganic electrolytes [17]. N,N-Dimethylacetamide (N,N-DMA) is a commodity chemical which is produced on a large scale and used in large quantities in any industries of fiber, pharmaceutical, pesticide, adhesive and battery for manufacture. Its high solubility in water and its excellent solvent power for high molecular weight polymers and resins make N,N-DMA a desirable solvent in fiber and polyurethane production. It is also a good reaction medium for the production of pharmaceuticals and cosmetics.

Like water, the amides have very high dielectric constants which make the two distinct media quite compatible. Hence the molecular complexity of the amide – water mixtures appears to be considerable in interactional and structural way [17]. In addition it is generally mixed with water at some point along the processes mentioned before. The resulting aqueous solutions are usually separated by a very energy intensive distillation process due to the high boiling point of N,N-DMA. The small impurities in these mixtures also lead to additional problems in distillation. Therefore, a process based on extraction of N,N-DMA from water using scCO_2 may be an attractive alternative to distillation.

2.1.3. Literature Examples of Removal of Organic Solvents from Aqueous Phase by Supercritical CO_2 Extraction

Supercritical CO_2 extraction is useful and effective method to remove commonly used solvents with different polarities from aqueous phase. The supercritical extraction of N,N-DMA is shown in Figure 2.2. In the supercritical extraction process firstly N,N-DMA aqueous solution is sent to the extractor and contacted with supercritical carbon dioxide. N,N-DMA is extracted from aqueous phase. Then N,N-DMA and CO_2 mixture is sent to the expansion valve to reduce the pressure and the solubility of N,N-DMA in CO_2. Hence N,N-DMA is separated as liquid phase and CO_2 is separated from as gaseous phase in the separator. Then CO_2 is used for recycle to the system and sent to the heat exchanger to reduce its temperature and to convert it to liquid phase and then it is pumped or compressed to another heat exchanger for increasing the temperature. After that CO_2 is used for another extraction in the system.

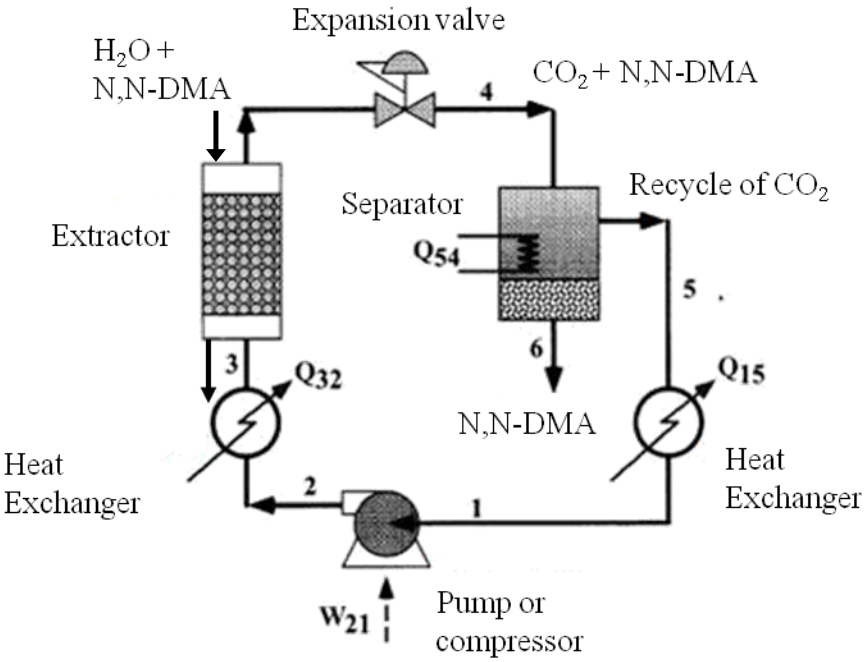

Figure 2.2 Schematic representation of supercritical fluid extraction

The supercritical fluid extraction (SFE) is a technology that is increasingly being used in commercial processes. In addition SFE is convenient for different media, including solids, natural products and liquid products. Supercritical CO_2 extraction is done at modestly low temperatures so this avoids any potential thermal decomposition of materials extracted under study. Supercritical fluids are used as solvents for numerous separation processes in industry because of their gas-like diffusivity, liquid-like density and zero surface tension. Also the CO_2 solvent strength can be easily tuned by adjusting the density of $ScCO_2$. Since CO_2 is gaseous in ambient temperature the extract can be concentrated by simply venting the final mixture to a cyclone collection vessel, using appropriate safety protocols [4,18,19].

Taylor has shown that SFE can be successfully used to extract a variety of organic compounds from aqueous phase. SFE of organic residues from aqueous streams has potential implications in the removal of the contaminants in drinking water and removal of commercial chemicals from waste streams [19,20,21,22].

Many studies of patent literature focus on the use of SFE for removing organic compounds from aqueous streams. Hardman made use of the fact that CO_2 forms a hexahydrate which serves to separate the aqueous phase from acrylic acid [23] and Shimshick recovered carboxylic acids from aqueous solutions of alkali metal salts via $scCO_2$ extraction. When the salt reacted with CO_2 an acid that dissolved in the supercritical phase was formed under these reaction conditions [24]. Bhise extracted ethylene oxide from a dilute aqueous phase using either $scCO_2$ or near $scCO_2$ [25]. DeFilippi developed a supercritical extractor, distillation unit and vapor recompressor for recovering organic solvents from aqueos stream [26]. Victor separated ethanol from aqueous phases using SFE techniques [27].

Leazer et al. studied the $scCO_2$ extraction of common organic solvents of varying polarities including toluene, tetrahydrofuran (THF), isopropyl acetate (IPAc), ethyl acetate (EtOAc), N -methyl-2-pyrrolidone (NMP), methyl tert-butyl ether (MTBE), and

acetonitrile (MeCN) from artificial aqueous waste streams for the waste management of the pharmaceutical industry [19].

Based on studies in the literature $scCO_2$ extraction which provides a green approach is convenient and effective in removing organic solvents from aqueous phase. SFE potentially leads to greener manufacturing processing because of being less energy intensive process in recent years.

2.1.4. Literature Examples of Phase Equilibria and Partition Coefficient of Organic Substances

The phase equilibria and the mass transfer characteristics of the systems which are extractions of organic substances from an aqueous solution by $scCO_2$ have to be determined accurately for the proper technical design. In order to characterize the phase equilibria, the partition coefficients have to be measured at different conditions. The partition coefficient, K_x, is defined as the ratio of molar fractions of a compound in both phases which are water and $scCO_2$ in equilibrium [1].

$$K_x = \frac{x_i^{scCO_2}}{x_i^{H_2O}} \tag{2.1}$$

Studies of supercritical extraction of organic compounds from aqueous phase have concentrated on a single-compound extraction. Akgerman determined the partition coefficients of benzene, toluene, naphthalene and parathion of a toxic organic mixture between water and $scCO_2$ phase and modeled the system that predicted the multicomponent system behavior. Akgerman found that the partition coefficients of organic compounds in six – component system were greater than those of compounds in ternary system [8].

Dahmen et al. studied the partitioning behaviour of phenol, benzoic acid, benzyl alcohol, 2-hexanone, vanillin and caffeine by developing a new apparatus for easy and

quick determination of partition coefficients between the temperature ranges of 313 to 333 K from 8 to 30 MPa. They measured the partition coefficients of phenol to check the reproducibility of the new apparatus and found the values between 0.2 and 1.5 that match in the literature data. They measured the partition coefficients of benzyl alcohol and benzoic acid between 0.4 and 2.7. The partition coefficients were obtained in the ranged from 10 and 140 for 2-hexanone, 0.02 to 0.25 for caffeine and 0.2 to 3 for vanillin [1]. Dahmen et al. measured the partition coefficients of aniline and benzaldehyde in the second part of this study. They measured the partition coefficients in the ranged of 0.21 to 3.03 for aniline and 2.5 to 62.9 for benzaldehyde. In addition they obtained the distribution behavior of a multicomponent mixture of phenol, benzyl alcohol, cyclohexanol and 2-hexanone. They found that the partition coefficients of alcohols was increased possibly by co-solubility of the 2-hexanone [28].

Tester et al. measured the partition coefficients of 18 different compounds including acetophenone, benzaldehyde, toluene and hexane at the temperature of 300 K and the pressure of 80 bar. They tested three different correlation methods to estimate the partition coefficients: first of them was the comparison to water solubility, second was the comparison to solvent/water partition coefficient and third was linear solvation energy relationship (LSER) estimations. They found that the LSER method was relatively strong with good agreement between measurements and predictions for all of 18 compounds [6].

2.2. Thermodynamics of Processes

The knowledge of thermodynamics of the system is important and essential for different processes when the pressure is close to the critical point of some of the components in the system. At these conditions, fluids behave as liquids according to their density in addition to that they have low viscosities and high diffusivities. These properties provide them to have superior mass transfer characteristics.

The solubility of a solute is changed exponentially in density such as very small variations in pressure cause large changes of solubility. This change can be explained with the high non-ideal thermodynamic behavior of mixtures. A small amount of a compound that is not close to its critical point can also have large effects on the solubility of a heavy compound in the high dense fluid. Another phenomena can be explained by the fact that the critical points for a mixture is not, as it happens for a pure compound, the maximum temperature and pressure that allows the coexistence of a vapor and a liquid phase in equilibrium.

In the case of extraction process of N,N-DMA from water with $scCO_2$, it is essential to determine the conditions at which N,N-DMA and carbon dioxide mixture is at a single phase and to determine the binary interaction parameters between of these compounds at the given conditions.

In the following sections, phase equilibrium with the guidance of Gibbs phase rule, phase equilibria calculations, and the equations of state will be described.

2.2.1. Phase Equilibrium

The behavior of the systems in phase equilibrium is an essential factor to determine the design and performance of components in the processes. Vapor-liquid equilibria (VLE) and vapor-liquid-liquid equilibria (VLLE) are the heart of the distillation processes, liquid-liquid equilibria (LLE) is important for extraction and liquid membrane separations.

When two phases are in equilibrium, the state of the system is fixed when only a single property is specified. For multi-phase systems this treatment should be extended to determine the minimum set of variables to describe the system both in extent and intensity. Postulate I: For closed simple systems with given internal restraints, there exist stable equilibrium states which can be characterized completely by two independently variable properties in addition to the masses of the particular chemical

species initially charged. When Postulate I is applied to each phase separately, one could choose any n+2 properties of each phase. For each phase a particularly convenient set of n+2 properties is;

$$T^{(s)}, P^{(s)}, x_1^{(s)}, \dots, x_{n-1}^{(s)}, N^{(s)} \tag{2.2}$$

For a multi-phase system containing π phases we have a set such as eq. (2.2) for each phase. The criteria of phase equilibria should be applied to determine which of π (n+2) properties are not independent. These properties are shown in the following for this system;

$$T^{(\alpha)} = T^{(\beta)} = \cdots = T^{(s)} = \cdots = T^{(\pi)} \tag{2.3}$$

$$P^{(\alpha)} = P^{(\beta)} = \cdots = P^{(s)} = \cdots = P^{(\pi)} \tag{2.4}$$

$$\mu_j^{\alpha} = \mu_j^{\beta} = \cdots = \mu_j^{(s)} = \cdots = \mu_j^{\pi} \quad (j = 1, \dots, n) \tag{2.5}$$

There are π -1 equalities in each of eqs.(2.3) and (2.4) and n(π-1) in eq.(2.5) for a total of (n+2)(π-1).

In conclusion, for a composite simple system containing π phases and n components in which chemical reactions do not occur, there are (n+2-π) independently variable intensive properties, and at least π extensive properties must be included in the set of n+2 properties necessary to describe the composite system completely. This result was first expressed by J. Willard Gibbs in 1875 and is referred ad the Gibbs phase rule. The phase rule is;

$$F = n + 2 - \pi \tag{2.6}$$

F is the number of degrees of freedom, n is the number of components and π is the number of phases. For a binary system, if a single phase exists then F=3 and one needs

a three dimensional T, P and x_i space to describe the system. In the same manner for a ternary system with single phase one needs a four dimensional T, P, x_1, x_2 space [29].

2.2.2. High-Pressure Phase Equilibria Calculations

The phase equilibria calculations are essential to predict the thermodynamics of the mixtures, to avoid direct experimental determinations. The choice of the appropriate thermodynamic model and parameters that are required for this model is the first and important requirement for the phase equilibria calculations. An equation of state is generally used to describe the properties of both phases at high pressure phase equilibria calculations. These equations of state will be explained in the next sections. In addition it is important to establish the stability of the system or the possibility that the system will split into two or more phases in equilibrium [30].

2.2.3. Calculations of Bubble Point, Dew Point and Flash

In order to solve the typical problems different combinations of the input variables are possible but the most commonly used are in the following [30]

- **Bubble Point Calculation**: For a liquid liquid mixture of given composition and at a given temperature / pressure, the pressure / temperature at which the first bubble of vapor phase appears and its composition is calculated.
- **Dew Point Calculation:** For a vapor mixture of a given composition and at a given temperature / pressure, the pressure / temperature at which the first drop of liquid phase appears and its composition is calculated.
- **Flash Calculation:** For a mixture of given global composition at given conditions of temperature and pressure it can be determined if the mixture is stable homogeneous liquid or vapor or that the mixture is heterogeneous and splits in a vapor phase and a liquid phase with different composition. If the

mixture is heterogeneous the composition and the amount of the vapor phase and of the liquid phase are calculated.

These calculations with an equation of state are iterative and performed by the simulations, and in the following sections the basic approach will be described.

2.2.4. Fugacity Coefficient and Activity Coefficient

The fugacity coefficient and the activity coefficient are commonly used in the thermodynamic calculations of phase equilibria. The fugacity function can be used instead of chemical potential to describe phase equilibrium. In addition, fugacity may be numerically determined at both low pressures and small concentrations.

The fugacity of a component i in a mixture, $\hat{f}_i$, is defined using the chemical potential as

$$\mu_i = RT ln\hat{f}_i + \lambda_i(T) \tag{2.7}$$

$\hat{f}_i$ is a function of temperature, pressure and composition. The circumflex ^ signifies that the fugacity applies to a component in a mixture. $\lambda_i(T)$ is a function of temperature and is specific for component i.

Since both pure substances and mixtures are assumed to approach an ideal-gas state as the pressure is decreased ($P \to P^* \approx 0$) then

$$\lim_{P \to P^*} \frac{\hat{f}_i}{y_i P} = 1 \tag{2.8}$$

In the case of an ideal gas $\hat{f}_i$ is equal to the partial pressure $P_i = y_i P$. The fugacity coefficient of a component, i, $\hat{\phi}_i$ is defined as

$$\hat{\phi}_i \equiv \frac{\hat{f}_i}{P_i} \tag{2.9}$$

The activity of a component i is defined as the ratio of fugacity in real state and fugacity in reference state which is denoted by superscript +;

$$a_i \equiv \frac{\hat{f}_i}{\hat{f}_i^{+}} \tag{2.10}$$

Note that the reference-state temperature is the same with the system temperature, but that the other reference state conditions, P^+, x_i^+, …, x_{n-1}^+ can be chosen arbitrarily. For the pure i reference state $x_i^+ = 1$. If the solution were ideal, then

$$a_i^{id} = x_i \text{ (ideal solution)} \tag{2.11}$$

The difference of the ratio from unity is a measure of the nonideality. This ratio is called the activity coefficient, γ_i, defined as,

$$\gamma_i \equiv \frac{\hat{f}_i}{\hat{f}_i x_i} \tag{2.12}$$

The activity coefficient represents the deviation of $\hat{f}_i$ from ideal solution. Also it can be calculated from a model for the molar excess Gibbs Energy, G^E

$$\ln \gamma_i \equiv \left[\frac{\partial \left(nG^E / RT \right)}{\partial n_i} \right]_{P,T,n_j} \tag{2.13}$$

The fugacity coefficients and activity coefficients of the compound in water and supercritical CO_2 system can be calculated by these definitions and equations to model the thermodynamics of the system [29,30].

2.2.5. Prediction of the Experimental Data and Modeling of the System

In the literature there are two different approaches to predict the experimental results of the partition coefficients of substances in water and supercritical CO_2 phase. One of them is linear solvation energy relationship (LSER) approach and the other one is modeling by Equations of State.

2.2.5.1 Linear Solvation Energy Relationship (LSER) Approach

Kamlet et al. developed the Quantitative structure – activity relationship (QSAR) theory in the form of a linear solvation energy relationship to predict the water-supercritical CO_2 partition coefficients for a published collection of data [31]. LSER methods involve the application of solvent parameters in linear or multiple-linear regression formulations to express solvent effects for property prediction and it has been used to model the properties of organic compounds in sc-CO_2 [32]. Lagalante and Bruno developed a model for the partition coefficients of organic solutes in the water-supercritical CO_2 system using LSER [33]. LSER models have potential to improve as the experimental database becomes larger and as theoretical methods are applied. However the prediction accuracy of LSER models is modest.

2.2.5.2 Equations of state

The equation of state is another approach to model the partition coefficients and the phase equilibria. It provides to describe the properties of phases. However when the critical point is approached the critical curves and solubility are very difficult to be predicted and correlated because of the nonclassical behavior in this region. The equations of state which are used to model the systems in the supercritical region are in the following [34]:

- The Van der Waals family of cubic equations of state
- The virial family of equations of state
- The group contribution equations of state
- Equations of state for associating and polar fluids
- Equations of state from theory and computer simulation

These calculations with an equation of state are iterative and performed by the simulations, and Van der Waals family of cubic equations of state will be explained in the following.

The ideal-gas law, which has both an empirical and theoretical basis, works well for fluids at low reduced densities ($\rho_r < 0.01$):

$$P = P^{ig} = \frac{RT}{v} \tag{2.14}$$

and 125 years ago van der Waals proposed his two parameter cubic equation of state:

$$P = \frac{RT}{v-b} - \frac{a}{v^2} \tag{2.15}$$

The vdW EOS can predict vapor liquid (VLE) for pure compounds at low densities. However its PVT predictions get considerably worse as the density of the fluid increases. Since this equation has only two parameters it predicts a universal value of the critical compressibility factor for all fluids. Introducing a third physical constant which is the acentric factor would moderate the restrictions of fixed critical compressibility factor. The different modifications of the vdW EOS have been published and three of them are given in Table 2.3. These modified equations of state give better predictions over a wide range of density.

Table 2.3 Commonly Used Equations of State for Pure Fluids [29]

Author	***Year***	***EOS***
Redlich and Kwong	1949	$P = \frac{RT}{v-b} - \frac{a(T)}{\sqrt{T}v(v+b)}$
Soave	1972	$P = \frac{RT}{v-b} - \frac{a(T)}{v(v+b)}$
Peng-Robinson	1976	$P = \frac{RT}{v-b} - \frac{a(T)}{v(v+b)+b(v-b)}$

Most of the EOSs used are explicit in pressure and are of the form as given in Table 2.3:

$$P = f(T, v, N) \tag{2.16}$$

Cubic equations of state have multiple volume or density roots and thus can be used to model both vapor and liquid phases. The modification of the vdW EOS by Redlich and Kwong [35] is very important since it opened the way to a better description of the temperature dependent properties like virial coefficients by introducing a different temperature and a slightly different volume dependency in the attractive term. The Redlich-Kwong equation gives a somewhat better critical compressibility but is still not very accurate for the prediction of densities.

Soave [36] modified the Redlich-Kwong EOS by introducing a dependence on the Pitzer acentric factor ω and changing the temperature dependence of the attractive term which resulted in accurate predictions of vapor-liquid equilibria at moderate and high pressures for non-polar fluids.

$$a = a_c f(\omega, T_r) = a_c (1 + k(1 - \sqrt{T_r}))^2 \tag{2.17}$$

$$k = 0.48508 + 1.55171\omega - 0.15613\omega^2 \tag{2.18}$$

These modifications greatly improved the accuracy of the Redlich-Kwong EOS for predicting liquid-vapor equilibria.

More accurate cubic EOS that can be applied to both the liquid and vapor regions was given by Peng and Robinson by using a different volume dependency of the attractive term. The parameters a and b in the PREOS are defined using critical point stability criteria. The attractive parameter depens on both the acentric factor and reduced temperature:

$$a(\omega, T_r) = a_c \alpha(\omega, T_r) \tag{2.19}$$

$$a_c = \frac{0.45724 R^2 T_c^2}{P_c} \tag{2.20}$$

$$\alpha(\omega, T_r) = (1 + \kappa(1 - \sqrt{T_r}))^2 \quad (2.21)$$

$$\kappa = 0.37464 + 1.54226\omega - 0.26992\omega^2 \quad (2.22)$$

$$b = \frac{0.07780RT_c}{P_c} \quad (2.23)$$

The cubic equations of state especially Peng-Robinson (PR) and the Redlich-Kwong-Soave (RKS) are most commonly used because they require little input information such as critical properties and acentric factor to calculate the generalized parameters and require little time for iteration. In addition RKS and PR EOSs treat the attractive interaction parameter as a function of temperature and so predict vapor pressure, enthalpy and entropy more accurately [29,30].

2.2.6. Methods for the Phase Equilibria and the Bubble Point Pressure Measurements

The phase behaviour of fluid mixtures at high pressure has received great attention over the past decade. However there is not a universal apparatus used for the measurement of the phase behavior for pure components and mixtures because of the wide variety of the properties of the compounds. Different types of apparatus have been developed for these measurements.

In the case of phase equilibria the typical set of data to be determined is the pressure, the temperature and the compositions of the phases at equilibrium. Many different reviews on apparatus developed and used for the measurements of the

thermodynamic properties of the mixtures at high pressure have been published [37,38,39,40].

There are mainly two different types of method which are static and dynamic methods in the literature [30,39,40]:

- Static Methods
  - Constant volume static cell (CVSC)
  - Variable volume static cell (VVSC)

- Dynamic Methods
  - Recirculation methods
  - Flow methods
  - Saturation methods

2.2.6.1 Principles of the Static Methods

The bubble point pressure measurements are carried out with constant composition expansion experiments in a temperature controlled pressure-volume-temperature (PVT) visual cell by static methods as shown in Figure 2.3. The mixture is placed into an evacuated cell, which is placed in a constant temperature bath (usually a liquid or air bath, although also metal-block thermostats have been used). The components separated into two or more phases of different densities are brought to equilibrium by shaking, stirring, or agitation by a magnetic stirrer. The static methods can be performed in constant volume static cell (CVSC) or in variable volume static cell (VVSC). In the VVSC, the pressure of the system can be increased slowly to a pressure above the bubble point and then decreased slowly by a movable piston until the first bubble is formed so the bubble point pressure can be recorded. The sample remains enclosed in the cell, because of dealing with a closed system, no phase or part of the system is subject to flow with respect to the others. In order to prevent or reduce the experimental

errors especially at high pressures in the reading of equilibrium pressure, the method requires careful evacuation of the cell and tubing and degassing of the materials.

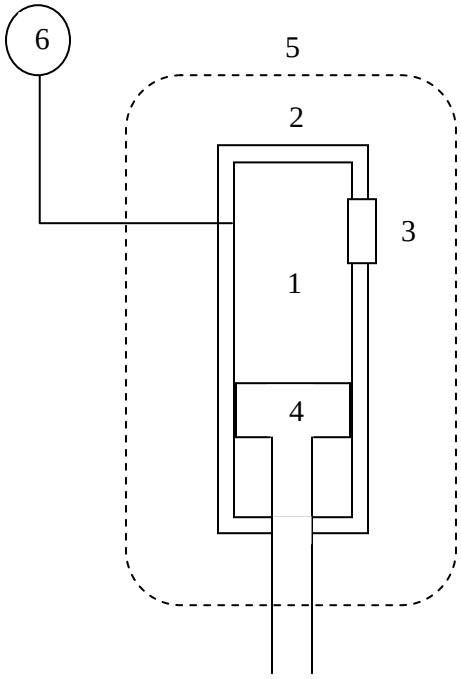

Figure 2.3 Schematic representation of Static Method: Variable volume static cell

1. mixture	4. free piston
2. equilibrium cell	5. thermostat
3. window	6. pressure gauge

In this method, known amounts of the pure substances are placed into the cell, so the overall composition of the mixture contained in the cell is known. The compositions of the co-existing equilibrium phases may be recalculated by iteration from the predetermined overall composition, and the equilibrium temperature and pressure data.

It is needed to know the pressure volume temperature (PVT) behavior as a function of the composition of phases in the form of a mathematical model which can be obtained by equations of state with sufficient accuracy. Sampling is accompanied by depressurization. The advantage of the static methods is that small amounts of substances are needed for the experiments [30].

2.2.6.2 Principles of the Dynamic Methods

The dynamic methods are developed from the static methods. The apparatus of the recirculation method which is one of the dynamic methods is shown in Figure 2.4. The main part of the apparatus is a thermostated equilibrium cell which is equipped with mechanically driven circulation through external loop(s) of either lighter (at the top) phase or the heavier (at the bottom) phase, or of both phases.

Introducing the external circulation of phases provides more efficient equilibration through stirring and contacting. So it improves the contact of phases and reduces the time required to reach equilibrium. After the equilibrium has been reached in steady-state conditions, the phases which are circulated through the external loop are already separated in equilibrium. In this method samples of the co-existing are withdrawn and analysed so that a known amount of sample is trapped in a sampling cell. The sampling cell can be removed for the analysis, or the sample may be temporarily circulated through an in-line sampling loop such as an injection valve, and then it is analyzed [30].

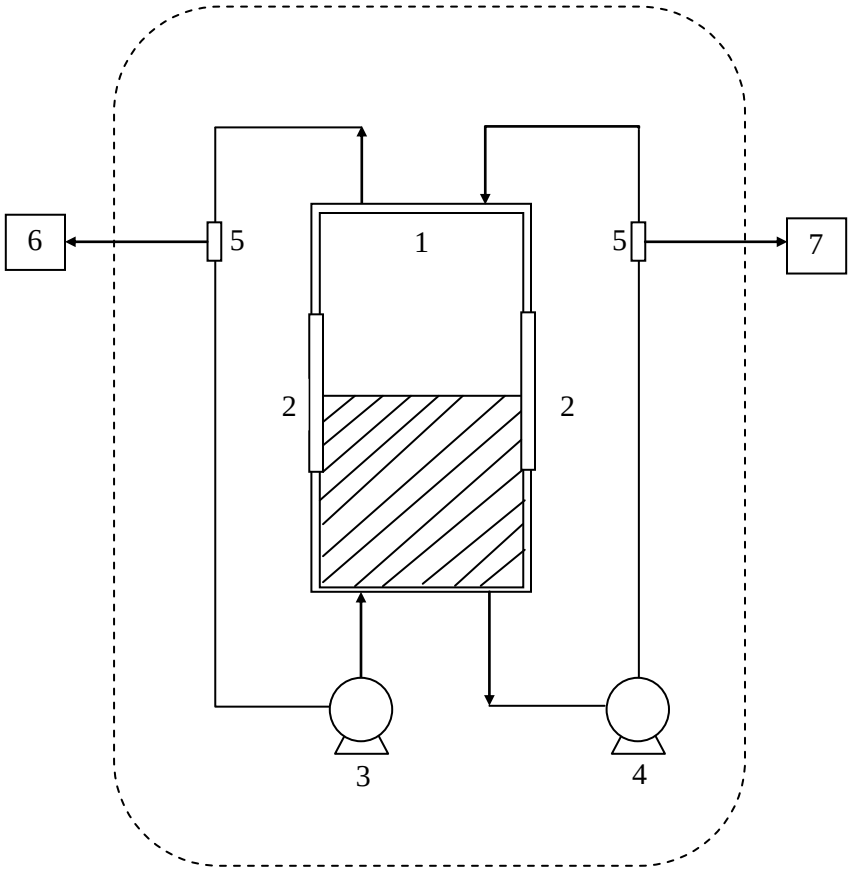

Figure 2.4: Schematic representation of Dynamic Method: Recirculation method

1. equilibrium cell
2. window
3. recirculation pump for vapor
4. recirculation pump for liquid
5. sampler
6. analysis for vapor
7. analysis for liquid

Chapter 3

EXPERIMENTAL SECTION

3.1 Materials

N,N-DMA was supplied by Merck (≥ 99% purity) and was used without further purification. Carbon dioxide (99.998%) was provided by Messer Aligaz. Water was deionized and distilled by DV 25 docking vessel of PURELAB Option-ELGA.

3.2 Experimental Methods

3.2.1 Apparatus and Procedure for Measuring the Partition Coefficients in N,N-Dimethylacetamide-Water-Carbon Dioxide System

The partition coefficients were measured using a static method in a stainless steel high-pressure vessel which had a working volume of 56 ml. The vessel was equipped with two sapphire windows (2.5 cm diameter, Sapphire Engineering, Inc., Pocasset; MA) for observation of the contents and sealed with polyether ether ketone o-rings. The experimental apparatus is shown in Figure 3.1. To determine the partition coefficients of N,N-DMA, a certain amount of aqueous solution of N,N-DMA was weighed and placed into the reaction vessel. Then the vessel brought to the working temperature by circulating water through the internal channels of the vessel by means of a circulating heater (Cole-Parmer Polystat Circulating Bath). To reach thermal equilibrium, the vessel was maintained at this temperature for a period of approximately 30 minutes. CO_2 was charged to the vessel up to the desired pressure by a syringe pump (Teledyne

ISCO Model: 260D) and then the vessel was isolated at these conditions. After equilibrium was achieved, samples were taken from the aqueous phase into a small vial by opening and closing the exit valve. The samples were diluted and analyzed afterwards by using a UV / VIS Spectrophotometer (UV-1700 PharmaSpec) to determine the composition of the sample. The amount of N,N-DMA in the $scCO_2$ phase was determined using the material balance for N,N-DMA. The pressure was measured by a pressure transducer (Omega Engineering Inc., model: PX4100-6KGV along with a meter - model: DP25B-S-230). The temperature of the system was measured by a thermocouple (Omega Engineering Inc., model: GTMQSS-062G-6 along with a meter - model: DP462) which was placed in a thermowell extending into the vessel. A magnetic stirrer was used to mix the contents. The partition coefficients were measured at different temperatures and pressures using aqueous solutions with various concentrations of N,N-DMA.

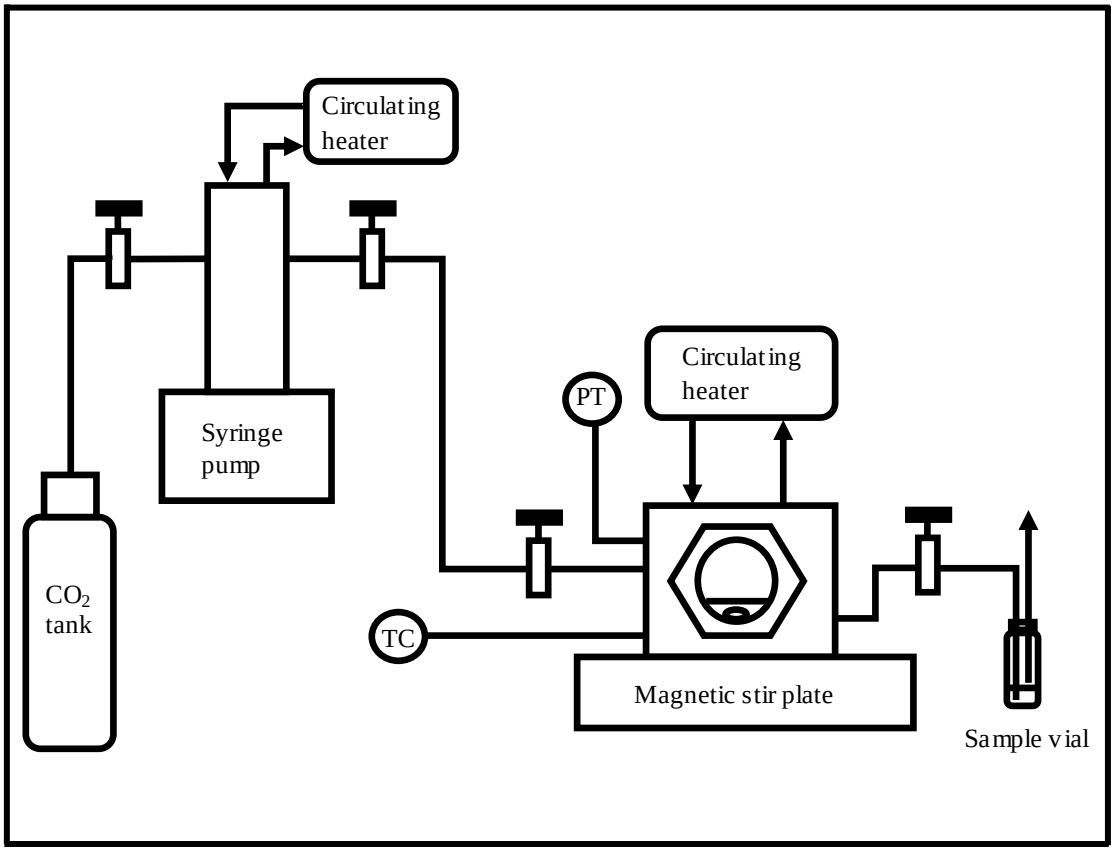

Figure 3.1: Experimental apparatus for supercritical extraction of N,N-DMA from aqueous phase.

The kinetics of extraction of N,N-DMA from water by $scCO_2$ was investigated using a N,N-DMA solution with an initial concentration of 4 wt % at 308.15 K and 24.1 MPa to determine how long it takes for the system to reach equilibrium. The kinetics was very rapid as shown in Figure 3.2. Hence, the contact time in all experiments was approximately 4 hours which was sufficient time to reach equilibrium.

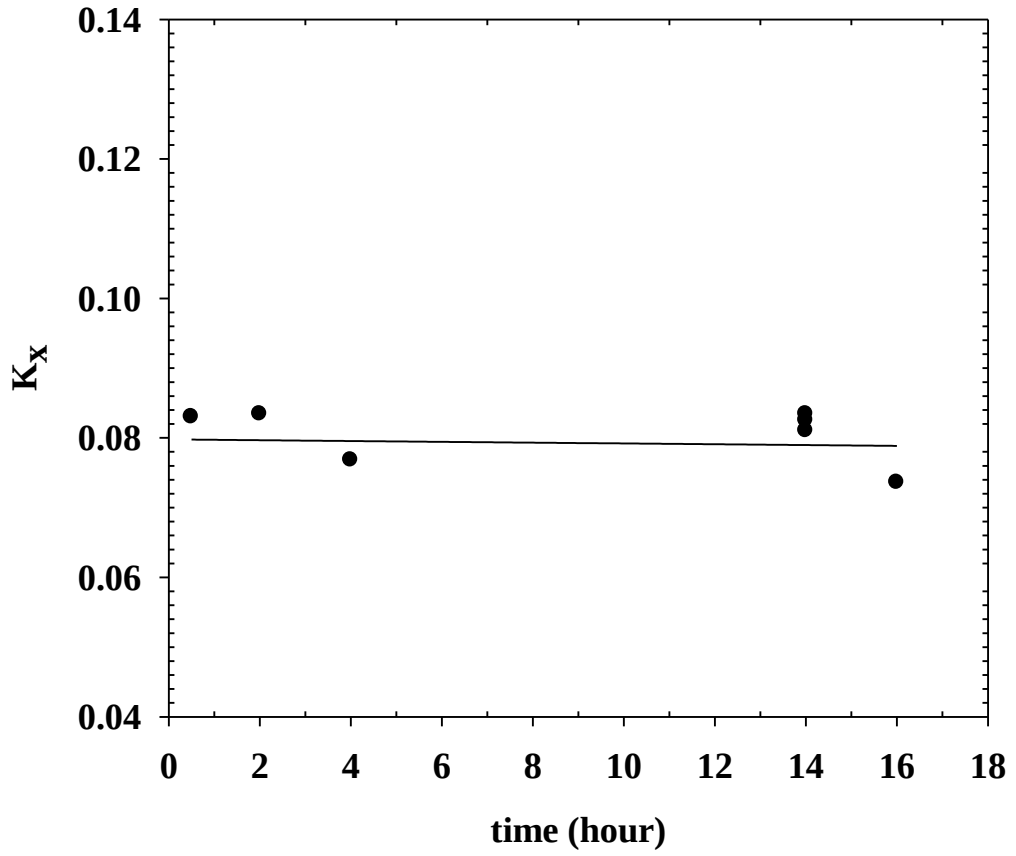

Figure 3.2: The kinetics of extraction of N,N-DMA from water by $scCO_2$.

3.2.1.1 Analysis of the Samples

The composition of the sample taken from the aqueous phase was determined by using the UV / VIS Spectrophotometer (UV-1700 PharmaSpec). The calibration curves were obtained by the solutions whose concentrations were 80, 100, 250, 500 and 1000 ppm. The absorbance values are in the range of 0.030 and 0.450. These absorbance values should not exceed the value of 1 because the higher values can cause errors in the analyzing. First the samples which were approximately 0.5 gram were diluted to 20

grams and 10 ml of this diluted sample was placed in a cuvette. Then they were analyzed by UV/ VIS Spectrophotometer at 235 nm of wavelength.

3.2.2 Apparatus and Procedure for the Bubble Point Pressure Measurements

The bubble point measurements of the binary mixture of N,N-DMA and CO_2 were carried out by the same apparatus used to measure the partition coefficients shown in Figure 3.1. For each measurement, a certain amount of N,N-DMA was weighed and placed into the high pressure vessel. At that point the system was seen from the view cell as shown in Figure 3.3.a. The vessel was then heated to the desired working temperature using the circulating heater (Cole-Parmer Polystat Circulating Bath). The system was maintained at this temperature for approximately 30 minutes to reach the thermal equilibrium. Subsequently, CO_2 was charged using the syringe pump (Teledyne ISCO Model: 260D) to a pressure high enough so that the mixture of N,N-DMA and CO_2 existed as a single phase as shown in Figure 3.3.b. Then the pressure of the system was slowly decreased until a second phase was observed at constant temperature as shown in Figure 3.3.c. This pressure at which a small bubble appeared in the vessel was recorded as the bubble point pressure.

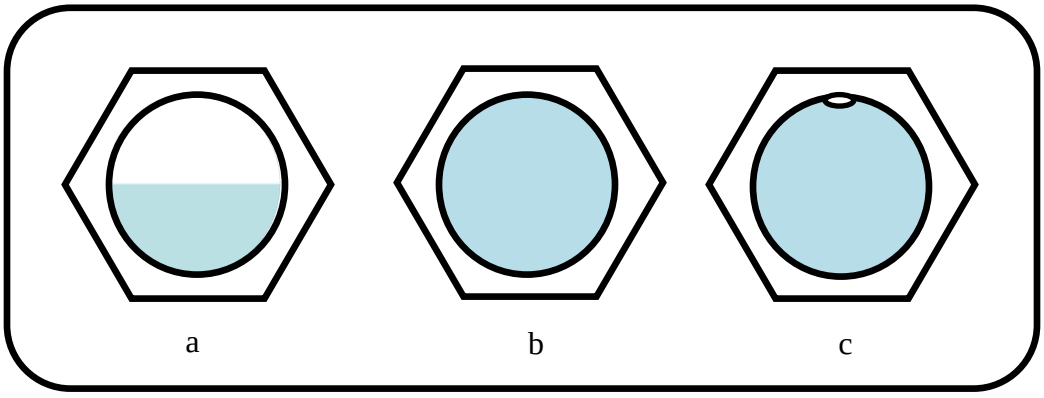

Figure 3.3: Phases during the bubble point measurements: a. at the initial b. at single phase (above the bubble point pressure) c. at the bubble point

3.2.2.1 N,N-DMA – CO_2 Solutions in Bubble Point Pressure Measurement

The mole fractions of N,N-DMA and CO_2 were obtained using the mass of N,N-DMA placed into the vessel and that of CO_2 loaded to the system which was determined as follows. The line from the syringe pump up to the high pressure vessel was charged with CO_2 to a pressure above the bubble point of the mixture of N,N-DMA and CO_2. The volume of CO_2 in the syringe pump was recorded. Subsequently, the inlet valve of the high pressure vessel was opened and the vessel was pressurized slowly until the desired pressure was reached. After closing the inlet valve, the volume of CO_2 in the pump was recorded. The volume of CO_2 loaded to the vessel was the difference between the initial and final values that were recorded. The mass of CO_2 used was determined using the volume and density of CO_2 at the pressure and temperature of the syringe pump. The temperature of the pump was kept constant at 298.15 K using a circulating heater (Cole-Parmer Polystat Circulating Bath). The density of CO_2 was calculated using a 52 parameter equation of state for CO_2 developed by IUPAC. The measurements were carried out using the same procedure for various temperatures (298.15 K, 308.15 K and 318.15 K) and compositions of the components.

Chapter 4

RESULTS AND DISCUSSION

4.1 Partition Coefficient Results

The partition coefficient is the ratio of the mole fraction of N,N-DMA in the supercritical phase to the mole fraction of N,N-DMA in the water phase at equilibrium.

$$K_x = \frac{y_i^{scCO_2}}{x_i^{H_2O}} \tag{4.1}$$

First, the dependence of the partition coefficient on the mole fraction of N,N-DMA in the aqueous phase was determined. The partition coefficients were measured using solutions with initial concentrations of 0.4, 1, 2, 5 and 10 wt % N,N-DMA at 308.15 K and 24.1 MPa. The partition coefficients increased from 0.08 to 0.11 by increasing mole fraction in the aqueous phase from 0.3 to 6.5 wt % as shown in Figure 4.1.

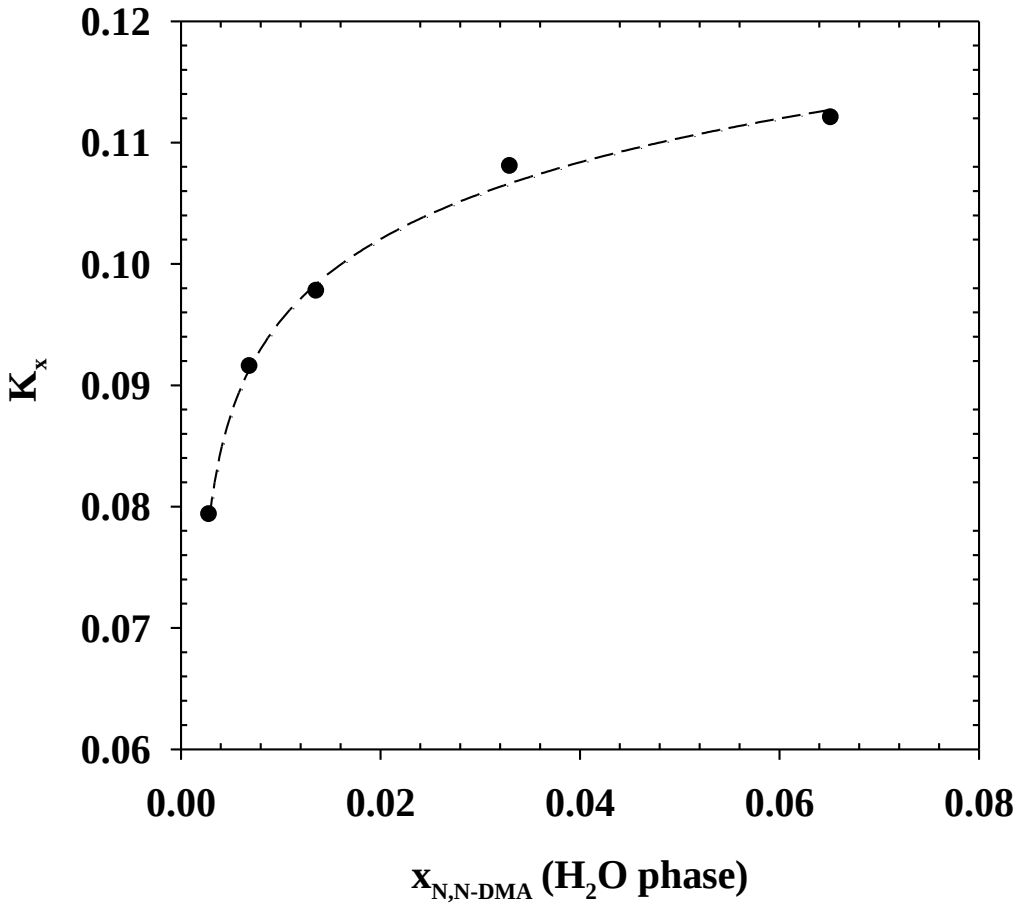

Figure 4.1: The partition coefficient values at different equilibrium mole fractions of N,N-DMA in aqueous phase

The partition coefficients were measured in the pressure ranges of 8.0 – 24.10 MPa and in the temperature range of 298.15 K – 328.15 K using 2 wt % aqueous solutions of N,N-DMA. The data are presented in Table 4.1. The partition coefficients increased with increasing pressure at a constant temperature because of the increasing solvent power of carbon dioxide with increasing pressure. At a particular pressure, the change of partition coefficients with temperature is more complex since an increase in temperature causes an increase in the vapor pressure of the solute but a decrease in the

density of the solvent.

Table 4.1 Partition Coefficient and mole fraction of N,N-DMA at various temperature, pressure and density of CO_2

Pressure (MPa)	ρ (g/cc)	K_x	$10^4 x_i^{CO_2}$
		T=298.15 K	
8.3	0.7867	0.0604	1.99
13.8	0.8664	0.0683	2.15
24.1	0.9391	0.0854	2.47
		T=308.15 K	
10.3	0.7289	0.0536	1.83
13.8	0.8002	0.0855	2.59
24.1	0.8968	0.0977	2.75
		T=318.15 K	
13.8	0.7186	0.0808	2.55
17.2	0.7809	0.0941	2.80
24.1	0.8516	0.1197	3.21
		T=328.15 K	
17.2	0.7116	0.1042	3.09
19.3	0.7471	0.1244	3.44
24.1	0.8040	0.1484	3.75

The influence of density on K_x is shown in Figure 4.2. At each temperature, the partition coefficients increased with increasing density. At a particular density, the partition coefficients increased with increasing temperature.

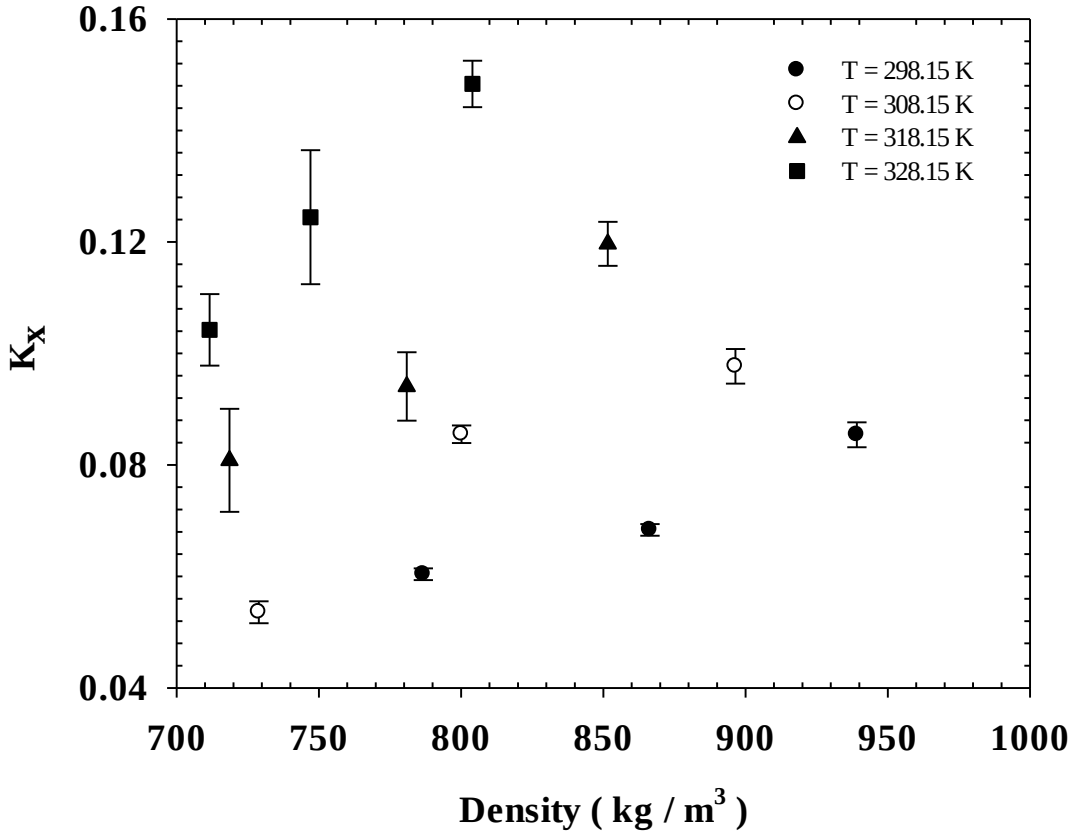

Figure 4.2: The change of partition coefficient with density of carbon dioxide

4.1.1 Testing for the accuracy of the partition coefficient data obtained by the experimental setup

Before conducting measurements on the partition coefficient, a set of experiments were carried out in order to test the accuracy of the measurement using our experimental setup. The experiments for the reproducibility were carried out at the temperature of 313 K and the pressure of 15.15 MPa. First, a known amount of benzaldehyde solution was placed inside the vessel. Then the vessel brought to the working temperature. After, CO_2 was charged to the vessel up to the desired pressure by the syringe pump. After equilibrium was achieved, samples were taken from the aqueous phase into a small vial by opening and closing the exit valve. The samples were diluted and analyzed afterwards using the UV/ VIS Spectrophotometer to determine the composition of the sample. The amount of benzaldehyde in the $scCO_2$ phase was determined using the material balance for N,N-DMA. The average of the measured values was 37.8 that was in good agreement with the value of 43.6 reported in the literature [28].

4.2 N,N-DMA – CO_2 Vapor Liquid Equilibria Results

The experimental pressure-composition (P – x) isotherms at 298.15, 308.15, and 318.15 K for N,N-DMA-CO_2 binary mixture are shown in Figure 5. At a constant temperature, the bubble point pressure of the mixture increased with increasing mole fraction of CO_2 in the binary mixture. At a fixed mole fraction of CO_2 the bubble point pressure of the mixture increased with an increase in temperature.

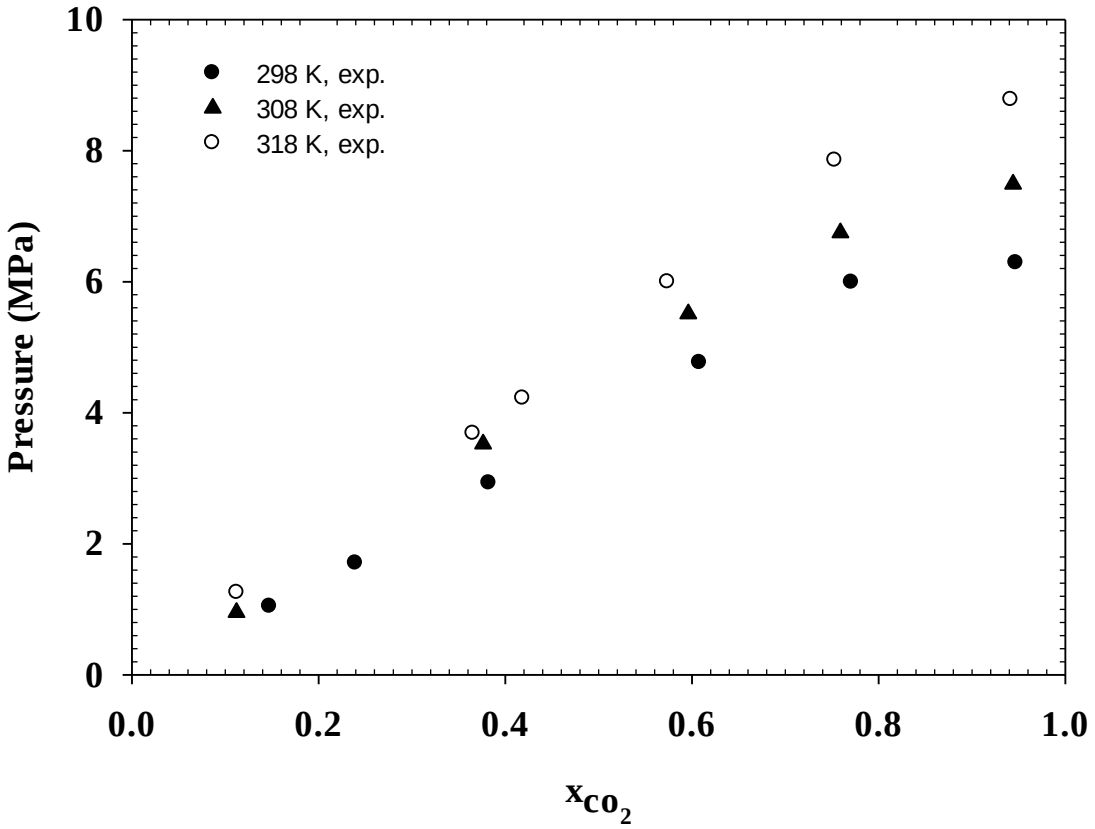

Figure 4.3: The bubble point pressure data for various temperatures and mole fraction of CO_2

4.2.1 Testing for the accuracy of the bubble point pressure measurements data obtained by the experimental setup

The accuracy of the experimental technique was tested by remeasurements of the bubble point pressures of the widely studied ethanol – CO_2 binary system at 333 K at the previous study [41]. The experimental data were in good agreement with the literature data [42,43,44].

4.3. Thermodynamic Modeling

For a species in equilibrium between two phases, the fugacity in the aqueous phase is equal to the fugacity in the $scCO_2$ phase at the same temperature and pressure as given by equation (2):

$$\hat{f}_i^{scCO_2} = \hat{f}_i^{H_2O} \tag{4.2}$$

which can be written as:

$$y_i^{scCO_2} \hat{\phi}_i^{scCO_2} P = x_i^{H_2O} \gamma_i^{H_2O} f_i \tag{4.3}$$

Therefore, the partition coefficient can be expressed as:

$$K_x = \frac{y_i^{scCO_2}}{x_i^{H_2O}} = \frac{\gamma_i^{H_2O} f_i}{\hat{\phi}_i^{scCO_2} P} \tag{4.4}$$

The fugacity coefficients were obtained using the Peng-Robinson Equation of State (PREOS) [45] given by:

$$P = \frac{RT}{v-b} - \frac{a(T)}{v(v+b)+b(v-b)} \tag{4.5}$$

The fugacity coefficient of N,N-DMA in vapor phase is related to PREOS by[46]:

$$\ln \hat{\phi}_i^V = \frac{1}{RT}\int_{\infty}^{V}\left[\frac{RT}{V} - N\left(\frac{\partial P}{\partial N_i}\right)_{T,V,N_{j\neq i}}\right]dV - \ln\frac{PV}{RT} \tag{4.6}$$

where ν is the molar volume, a is the attraction parameter and b is van der Waals covolume parameter. The Panagiotopoulos and Reid mixing rule was utilized which is given by:

$$\mathrm{a} = \sum_{\mathrm{i}}\sum_{\mathrm{j}} \mathrm{x_i x_j a_{ij}} \tag{4.7}$$

$$b = \sum_i x_i b_i \tag{4.8}$$

$$a_{ij} = \sqrt{a_i a_j}\left(1 - K_{ij}\right) \tag{4.9}$$

$$K_{ij} = k_{ij} - \left(k_{ij} - k_{ji}\right)x_i \quad \text{with } k_{ij} \neq k_{ji} \tag{4.10}$$

where k_{ij} and k_{ji} are binary interaction parameters. The parameters a and b for pure components are expressed by:

$$a_i = 0.45724 \frac{\alpha(T_{ri}, w_i) R^2 T_{ci}^2}{P_{ci}} \quad (4.11)$$

$$b_i = 0.07780 \frac{RT_{ci}}{P_{ci}} \quad (4.12)$$

where

$$\alpha^{1/2} = 1 + \kappa\left(1 - \sqrt{T_{ri}}\right) \quad (4.13)$$

$$\kappa = 0.37464 + 1.54226\omega - 0.26992\omega^2 \quad (4.14)$$

T_{ri} is the reduced temperature given by $T_{ri} = T/T_{ci}$. The critical temperature (T_c), critical pressure (P_c) and acentric factor (ω) of N,N-DMA, water and CO_2 are reported in Table 4.2.

Table 4.2 Pure component parameters used in PREOS [47]

Component	Formula	MW (g/mol)	T_c (K)	P_c (MPa)	Acentric factor, ω
Carbon dioxide	CO_2	44.01	304.19	7.382	0.228
N,N-DMA	C_4H_9NO	87.12	658.00	4.030	0.364
Water	H_2O	18.01	647.13	22.055	0.345

The activity coefficients for N,N-DMA – water mixtures were obtained using the Redlich – Kister equation [48] given as:

$$G^E/RT = Q = x(1-x)\sum_{i=1}^{N} C_i (2x-1)^{i-1} \tag{4.15}$$

where N is the number of adjustable parameters and x is the mole fraction of N,N-DMA in the water phase. The constants in equation (4.15) are given in Table 4.3[49].

Table 4.3 The constants for Redlich – Kister equation [49]

Constants	C_1	C_2	C_3	C_4
	– 0.608830	0.280078	– 0.021106	– 0.021106

The activity coefficient is related to G^E/RT by:

$$\ln \gamma_i = \left[\frac{\partial (nG^E / RT)}{\partial n_i} \right]_{P,T,n_j} \tag{4.16}$$

Water is partially miscible with carbon dioxide and the CO_2 phase was assumed saturated with water. The binary interaction parameters for the CO_2 – H_2O pair were taken from the literature [50]. The binary interaction parameters for CO_2 – N,N-DMA system and H_2O – N,N-DMA system were determined by minimizing the objective function:

$$O.F. = \sum_{i=1}^{n} \left[\left(K_i^{\exp} - \frac{\gamma_i^{calc} f_i^{calc}}{\hat{\phi}_i^{calc} P} \right)^2 \right] \tag{4.17}$$

The binary interaction parameters of the binary pairs of N,N-DMA – CO_2 – H_2O are given in Table 4.4. The model predictions given by solid and dashed lines in Figure 4.4 show that the agreement between the model and the data are good with an average absolute percent error of 14.3. The effect of the binary interaction parameter of the N,N-DMA - water pair was also found to be very small.

Table 4.4 Binary interaction parameters for CO_2 (1) – N,N-DMA (2) – H_2O (3) system

Binary System	k_{ij}	k_{ji}
CO_2 (1) + N,N-DMA (2)	$-0.3705 + 1.0039 \times 10^{-3}T$	$0.4249 + (-1.4106 \times 10^{-3}T)$
CO_2 (1) + H_2O (3) [14]	$-0.4271 + 1.0377 \times 10^{-3}T$	$-0.4516 + 1.9813 \times 10^{-3}T$
N,N-DMA (2) + H_2O (3)	– 0.0724	0.0213

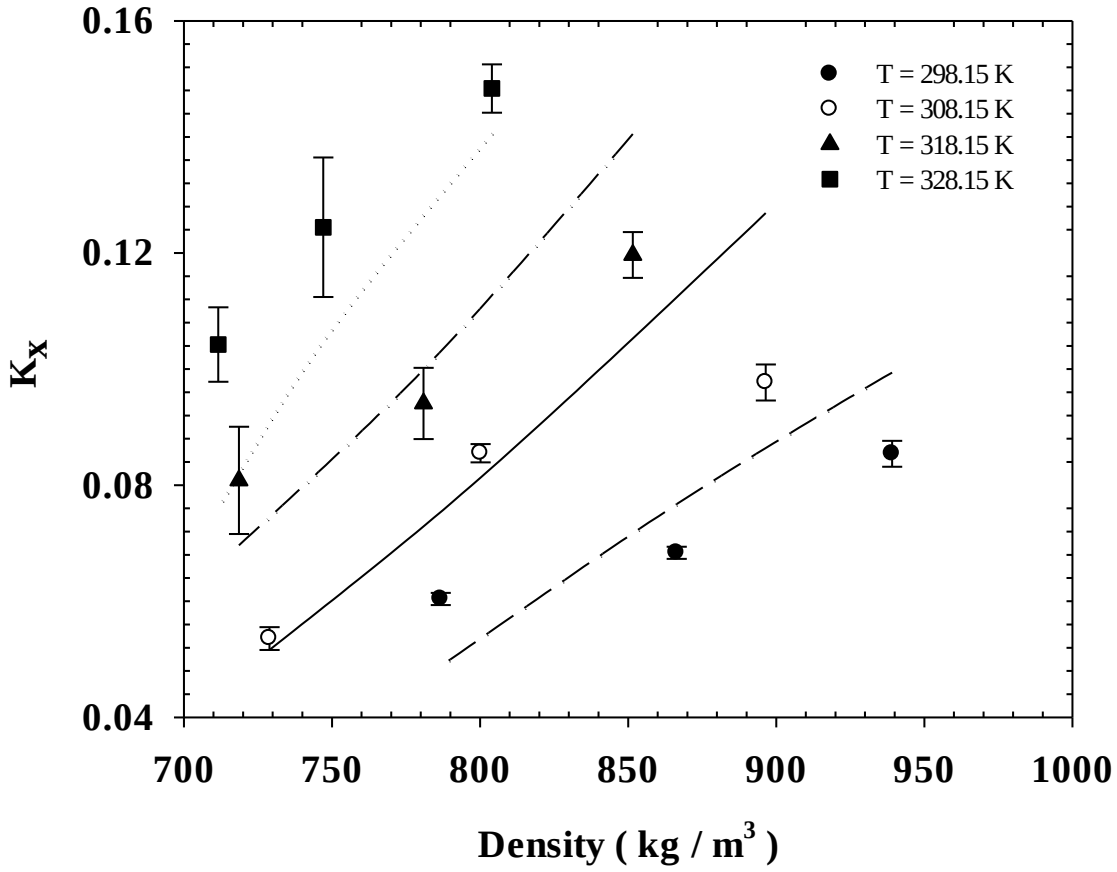

Figure 4.4 The comparison between the predicted and experimental data of partition Coefficients

4.3.1 Bubble Point Pressure Calculations

The starting point of phase equilibrium calculations is the equality of fugacity of species in each phase at the same temperature and pressure as given in section 4.3:

$$\hat{f}_i^L(T,P,x) = \hat{f}_i^V(T,P,y) \tag{4.18}$$

$$y_i\hat{\phi}_i^v = x_i\hat{\phi}_i^l \tag{4.19}$$

Bubble point pressure calculations with Peng Robinson Equation of State are iterative and sufficiently complicated to best be done on computer program. The algorithm of the bubble point pressure calculations are shown in Figure 4.5. For each iterative calculation for a liquid of a known composition, x_i, at a known temperature, T, vapor phase composition, y_i, and the bubble point pressure, P, must be guessed initially.

Using this vapor phase composition guessed the equation of state parameters given in section 4.3 and fugacity coefficients for each phase are reevaluated with the EOS parameters as given:

$$\ln\hat{\phi}_i^V = \frac{b_i}{b}\left(Z^v - 1\right) - \ln\left(Z^v - B\right) - \frac{A}{2\sqrt{2}B}\left(\frac{2\sum_i y_i a_{ij}}{a} - \frac{b_i}{b}\right)\ln\left(\frac{Z^v + 2.414B}{Z^v - 0.414B}\right) \tag{4.20}$$

$$\ln\hat{\phi}_i^L = \frac{b_i}{b}\left(Z^l - 1\right) - \ln\left(Z^l - B\right) - \frac{A}{2\sqrt{2}B}\left(\frac{2\sum_i x_i a_{ij}}{a} - \frac{b_i}{b}\right)\ln\left(\frac{Z^l + 2.414B}{Z^l - 0.414B}\right) \tag{4.21}$$

$$A = \frac{aP}{R^2 T^2} \tag{4.22}$$

$$B = \frac{bP}{RT} \tag{4.23}$$

$$Z = \frac{P\upsilon}{RT} \tag{4.24}$$

$$y_i = x_i \frac{\hat{\phi}_i^l}{\hat{\phi}_i^v} = x_i K_i \tag{4.25}$$

Since $\sum_i y_i = 1$ ($y_1 + y_2 = 1$ for a binary mixture), the equation should hold for a binary mixture at the equilibrium

$$\sum_i K_i x_i = 1 \tag{4.26}$$

Therefore,

$$K_1 x_1^{H_2O} + K_2 x_2^{H_2O} = 1 \tag{4.27}$$

After the fugacity coefficient are reevaluated, $\sum_i K_i x_i$ is checked if it changes or not. If the results are not satisfied, the vapor phase composition is reevaluated given by the normalizing equation:

$$y_i = \frac{K_i x_i}{\sum_i K_i x_i} \tag{4.28}$$

This method is repeated until two successive values of $\sum_i K_i x_i$ are equal to each other. When the equal values of $\sum_i K_i x_i$ are obtained, the results are checked to see $\sum_i K_i x_i = 1$. If this condition is not achieved, a new pressure value is guessed and the same procedure is repeated until the bubble pressure is found. If the condition is achieved, the assumed pressure is concluded as the bubble point pressure [46,51].

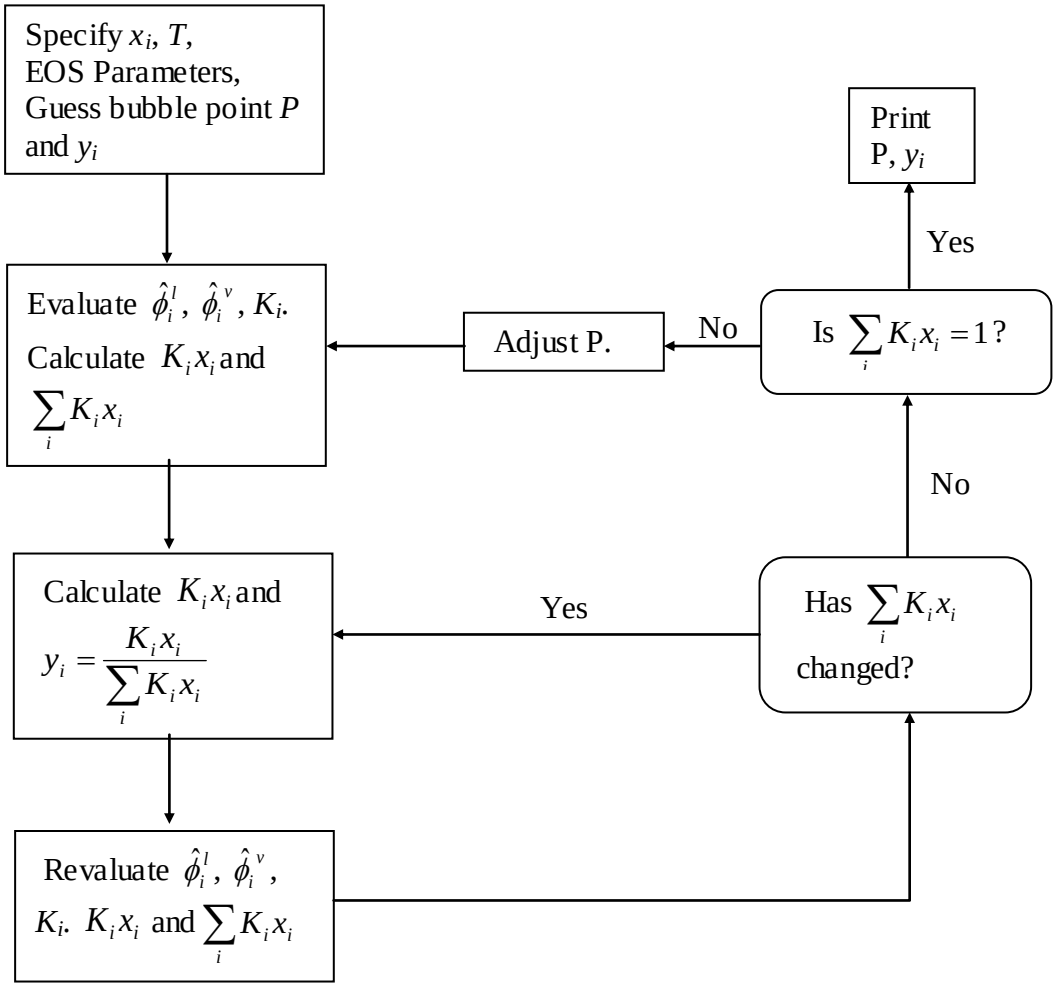

Figure 4.5 Algorithm for the bubble point pressure calculation [51]

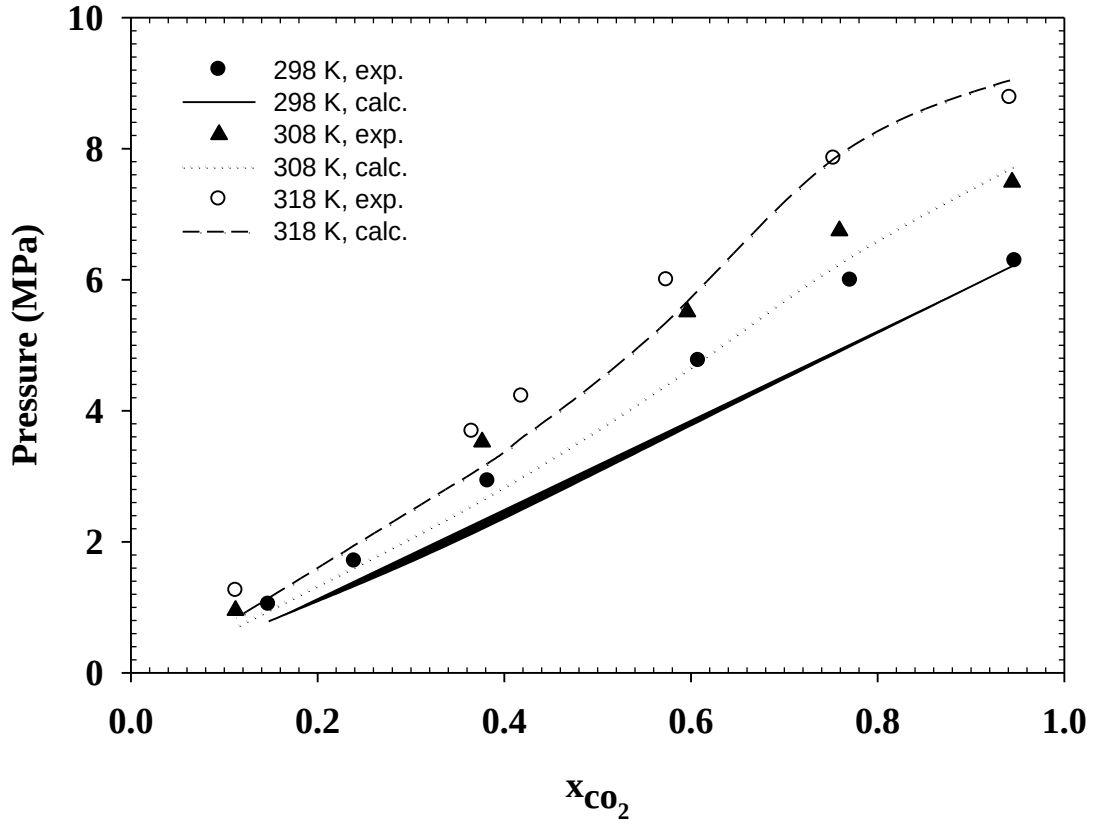

Figure 4.6: The comparison of calculated and experimental data of the bubble point pressure for various temperatures and mole fraction of CO_2

During these calculations the binary interaction parameters regressed from the partition coefficient data were used to predict the bubble point pressures. A comparison between the experimental bubble point pressures for CO_2 – N,N-DMA and predictions obtained using the PREOS is shown in Figure 4.6. The average absolute deviation (AAD) was 17.90 % at 298.15 K, 15.50 % at 308.15 K and 13.27 % at 318.15 K.

Chapter 5

CONCLUSIONS

The partition coefficients of N,N-DMA between water and scCO_2 were measured in the temperature range of 298.15 K – 318.15 K and in the pressure range of 80 – 240 atm. The partition coefficients increased with increasing pressure at a fixed temperature and increased with increasing at a constant density. They were found to depend on the mole fraction of N,N-DMA in the aqueous phase and increased with increasing mole fraction. The partition coefficients were modeled using the PREOS with modified van der Waals mixing rule – the Panagiotopoulos and Reid mixing rule. The binary interaction parameters for N,N-DMA – CO_2 pair regressed from experimental data were found to depend linearly on temperature.

Furthermore, the bubble point pressures of binary mixtures of N,N-DMA and CO_2 were determined for various mole fractions and at different temperatures. The bubble point pressures increased with increasing mole fraction of CO_2 at constant temperature and increased with increasing temperature at constant composition. PREOS was found to predict the experimental data with binary interaction parameters regressed from partition coefficient data by using computer simulation.

APPENDIX 1

THERMODYNAMIC MODELING

MATLAB Programme

1.1 Calculations for the Activity Coefficient

```
clear all;
close all;
clc;


%%%%%%%SATURATION%%%%%%%%%%

Tc=658;           % in K
Pc=40.3;          % in bar
om=0.3635;        % acentric factor at Tr=0.7;

P=83 ;            % pressure of the system in bar
T=298.2;          % temperature of the system, in K
R=83.1447;        % gas constant, cm^3*bar/(mol*K)

%%%%%% Psaturation with Antoine equation %%%%%%

An=3.08664;
Bn=391.115;
Cn=194.054;
Psat=(10^(An-Bn/(T-Cn)))/100  % of DMAc in bar

%%%%% physical properties of N,N-DMA %%%%%%
ro=0.937          % g/ml at 298.15 K
M=87.12           %g/mol


aTc=0.45724*R^2*Tc^2/Pc;
bTc=0.07780*R*Tc/Pc;
kappa=0.37464+1.54226*om-0.26992*om^2;
Tr=T/Tc;
alpha=(1+kappa*(1-Tr^0.5))^2;
```

```
aT=aTc*alpha;
bT=bTc;

A=aT*Psat/(R*T)^2;
B=bT*Psat/(R*T);

s1=1;
s2=-(1-B);
s3=A-3*B^2-2*B;
s4=-(A*B-B^2-B^3);
px=[s1 s2 s3 s4];
Zx=roots(px)


v=0;
for q=1:3
    TF=isreal(Zx(q));
    if TF==1
        v=v+1;
        Zliq(v)=Zx(q);
    end;
end;
Z=max(Zliq)


%%%%% poynthing factor %%%%%%%%%%
Vi=M/ro
Pf=exp(Vi*(P-Psat)/(R*T))
%%%%%%%%%%%%%%%%%%%%%%%%%%%%%%%%

Phisat=exp(Z-1-log(Z-B)-A/(2*2^0.5*B)*log((Z+2.414*B)/(Z-0.414*B)))
fi=Phisat*Psat*Pf
%%%%%%%%%%%%%%%%%%%%%%%%%%%%%%%%%%%%


%%%%% ACTIVITY COEFFICIENT %%%%%
% T= 35 C & P= 83 bar

x1=0.003298347;
x2=1-x1;

m1=(-0.608830+0.280078*(x1-x2)-0.021106*(x1-x2)^2-0.021106*(x1-x2)^3);
m2=(0.280078-0.280078*(x1-x2)+2*(-0.021106)*(x1-x2)-2*(-0.021106)*(x1-
x2)^2+3*(-0.021106)*(x1-x2)^2-3*(-0.021106)*(x1-x2)^3);

gamma=exp(x2*m1-x1*x2*m1+x1*x2*m2)
```

1.2 Calculations for Fugacity Coefficient and Binary Interaction Parameters

```
clear all;
close all;
clc;


A0=[-0.3705;1.004e-3;0.4249;-1.4e-3]
options=optimset('Display','iter'); %,'TolFun',1e-10
[A,fval,exitflag] = fsolve(@myfun328li,A0,options)
Texp=[298.15 308.15 318.15 328.15];
k12exp=[A(1)+A(2)*Texp(1) A(1)+A(2)*Texp(2) A(1)+A(2)*Texp(3)
A(1)+A(2)*Texp(4)]
k21exp=[A(3)+A(4)*Texp(1) A(3)+A(4)*Texp(2) A(3)+A(4)*Texp(3)
A(3)+A(4)*Texp(4)]
fprintf('A(1)= %7.7f\n',A(1));
fprintf('A(2)= %7.7f\n',A(2));
fprintf('A(3)= %7.7f\n',A(3));
fprintf('A(4)= %7.7f\n',A(4));




%%%%% FUGACITIY %%%%%%

function F = myfun328li(A0)
% Component properties
% 1-CO2 2-DMAC 3-H2O
Tc=[304.19
    658
    647.13];            % in K
Pc=[73.82
    40.3
    220.55];            % in bar
om=[0.23
    0.3635
    0.345];             % acentric factor

%%% 1.   298 K ALL PRESSURES

T1=298.2;               % temp. of system, in K
R=83.1447;              % gas constant, cm3*bar/(mol*K)
```

```
for i=1:3
    aTc(i)=0.45724*R^2*Tc(i)^2/Pc(i);
    bTc(i)=0.07780*R*Tc(i)/Pc(i);
    kappa(i)=0.37464+1.54226*om(i)-0.26992*om(i)^2;
    Tr1(i)=T1/Tc(i);
    alpha1(i)=(1+kappa(i)*(1-(Tr1(i))^0.5))^2;
    aT1(i)=aTc(i)*alpha1(i);
    bT(i)=bTc(i);
end;

% FOR 83 BAR

x2=0.000199357;          % mole fraction of DMAc
x3=0.004;                % mole fraction of H2O fron K=0.0040
x1=1-x2-x3;              % mole fraction of CO2

P1=83;                   % pressure of system in bar


%%%% for 1-CO2 - 2-DMAC %%%%%%%
k12=A0(1)+A0(2)*T1;
k21=A0(3)+A0(4)*T1;
a12=(aT1(1)*aT1(2))^(1/2)*(1-k12+x1*(k12-k21));
%%%%a12 =1.5131e+007

%%%% for 1-CO2 - 3-H20 %%%%%%%
k13=-0.4271+1.0377e-3*T1;     %from Maurer
k31=-0.4516+1.9813e-3*T1;     %from Maurer
a13=(aT1(1)*aT1(3))^(1/2)*(1-k13+x1*(k13-k31));


%%%% for 2-DMAC - 3-H20 %%%%%%%
k23=-0.0724;
k32=0.0213;
a23=(aT1(2)*aT1(3))^(1/2)*(1-k23+x2*(k23-k32));


a1=x1*x1*aT1(1)+x2*x2*aT1(2)+x3*x3*aT1(3)+2*x1*x2*a12+2*x1*x3*a13+2*x2
*x3*a23;
b1=x1*bT(1)+x2*bT(2)+x3*bT(3);


A1=a1*P1/(R*T1)^2;
B1=b1*P1/(R*T1);
```

```
s1=1;
s2=-(1-B1);
s3=A1-3*B1^2-2*B1;
s4=-(A1*B1-B1^2-B1^3);
px=[s1 s2 s3 s4];
Zx=roots(px)
v=0;
for q=1:3
    TF=isreal(Zx(q));
    if TF==1
        v=v+1;
        Zvap(v)=Zx(q);
    end;
end;
Z1=max(Zvap)

Kexp1=0.060452;
gamma1=0.4149;
fi1=0.0029;



%%%%%%%%% FOR 138 BAR %%%%%%%%%%%%%%%%%%%%

x22=0.000214791;              % mole fraction of DMAc
x23=0.004;                    % mole fraction of H2O from K=0.0040
x21=1-x22-x23;                % mole fraction of CO2

P2=138;                       % pressure of system in bar


%%%% for 1-CO2 - 2-DMAC %%%%%%%

c12=(aT1(1)*aT1(2))^(1/2)*(1-k12+x21*(k12-k21));


%%%% for 1-CO2 - 3-H20 %%%%%%%

c13=(aT1(1)*aT1(3))^(1/2)*(1-k13+x21*(k13-k31));


%%%% for 2-DMAC - 3-H20 %%%%%%%

c23=(aT1(2)*aT1(3))^(1/2)*(1-k23+x22*(k23-k32));


c1=x21*x21*aT1(1)+x22*x22*aT1(2)+x23*x23*aT1(3)+2*x21*x22*c12+2*x1*x3*
c13+2*x2*x3*c23;
```

```
d1=x21*bT(1)+x22*bT(2)+x23*bT(3);


C1=c1*P2/(R*T1)^2;
D1=b1*P2/(R*T1);



s21=1;
s22=-(1-D1);
s23=C1-3*D1^2-2*D1;
s24=-(C1*D1-D1^2-D1^3);
px2=[s21 s22 s23 s24];
Zx2=roots(px2)
v=0;
for q=1:3
    TF=isreal(Zx2(q));
    if TF==1
        v=v+1;
        Zvap(v)=Zx2(q);
    end;
end;
Z2=max(Zvap)

Kexp2=0.068339;
gamma2=0.4147;
fi2=0.0036;

%%%%%%%%%%%%% FOR 241 BAR %%%%%%%%%%

x32=0.000247404;              % mole fraction of DMAc
x33=0.004;                    % mole fraction of H2O from K=0.0040
x31=1-x32-x33;                % mole fraction of CO2

P3=241; % pressure of system in bar( 1200,2000,3500psi)


%%%% for 1-CO2 - 2-DMAC %%%%%%%

e12=(aT1(1)*aT1(2))^(1/2)*(1-k12+x31*(k12-k21));


%%%% for 1-CO2 - 3-H20 %%%%%%%

e13=(aT1(1)*aT1(3))^(1/2)*(1-k13+x31*(k13-k31));


%%%% for 2-DMAC - 3-H20 %%%%%%%
```

```
e23=(aT1(2)*aT1(3))^(1/2)*(1-k23+x32*(k23-k32));


e1=x31*x31*aT1(1)+x32*x32*aT1(2)+x33*x33*aT1(3)+2*x31*x32*e12+2*x31*x3
3*e13+2*x2*x3*e23;
f1=x31*bT(1)+x32*bT(2)+x33*bT(3);


E1=e1*P3/(R*T1)^2;
F1=f1*P3/(R*T1);



s31=1;
s32=-(1-F1);
s33=E1-3*F1^2-2*F1;
s34=-(E1*F1-F1^2-F1^3);
px3=[s31 s32 s33 s34];
Zx3=roots(px3)
v=0;
for q=1:3
    TF=isreal(Zx3(q));
    if TF==1
        v=v+1;
        Zvap(v)=Zx3(q);
    end;
end;
Z3=max(Zvap)

Kexp3=0.085402;
gamma3=0.4145;
fi3=0.0053;

%%% 2.   308 K ALL PRESSURES

T2=308.2;         % temperature of the system, in K

for i=1:3
    aTc(i)=0.45724*R^2*Tc(i)^2/Pc(i);
    bTc(i)=0.07780*R*Tc(i)/Pc(i);
    kappa(i)=0.37464+1.54226*om(i)-0.26992*om(i)^2;
    Tr2(i)=T2/Tc(i);
    alpha2(i)=(1+kappa(i)*(1-(Tr2(i))^0.5))^2;
    aT2(i)=aTc(i)*alpha2(i);
    bT(i)=bTc(i);
end;

% FOR 103 BAR
IIx2=0.000183392;            % mole fraction of DMAc
```

```
IIx3=0.004;                    % mole fraction of H2O from K=0.0040
IIx1=1-IIx2-IIx3;              % mole fraction of CO2

IIP1=103; % pressure of system in bar

%%%% for 1-CO2 - 2-DMAC %%%%%%%

IIk12=A0(1)+A0(2)*T2;
IIk21=A0(3)+A0(4)*T2;
IIa12=(aT2(1)*aT2(2))^(1/2)*(1-IIk12+IIx1*(IIk12-IIk21));

%%%% for 1-CO2 - 3-H20 %%%%%%%
IIk13=-0.4271+1.0377e-3*T2;   %from Maurer
IIk31=-0.4516+1.9813e-3*T2;   %from Maurer
IIa13=(aT2(1)*aT2(3))^(1/2)*(1-IIk13+IIx1*(IIk13-IIk31));

%%%% for 2-DMAC - 3-H20 %%%%%%%

IIa23=(aT2(2)*aT2(3))^(1/2)*(1-k23+IIx2*(k23-k32));

a2=IIx1*IIx1*aT2(1)+IIx2*IIx2*aT2(2)+IIx3*IIx3*aT2(3)+2*IIx1*IIx2*IIa1
2+2*IIx1*IIx3*IIa13+2*IIx2*IIx3*IIa23;
b2=IIx1*bT(1)+IIx2*bT(2)+IIx3*bT(3);

A2=a2*IIP1/(R*T2)^2;
B2=b2*IIP1/(R*T2);

IIs1=1;
IIs2=-(1-B2);
IIs3=A2-3*B2^2-2*B2;
IIs4=-(A2*B2-B2^2-B2^3);
IIpx=[IIs1 IIs2 IIs3 IIs4];
IIZx=roots(IIpx)
IIv=0;
for q=1:3
    TF=isreal(IIZx(q));
    if TF==1
        IIv=IIv+1;
        IIZvap(IIv)=IIZx(q);
    end;
end;
IIZ1=max(IIZvap)

IIKexp1=0.0536;
IIgamma1=0.4151;
IIfi1=0.0066;
```

```
%%%%%%%%%%% FOR 138 BAR %%%%%%%%%

IIx22=0.000259124;            % mole fraction of DMAc
IIx23=0.004;                  % mole fraction of H2O fron K=0.0040
IIx21=1-IIx22-IIx23;          % mole fraction of CO2

IIP2=138;          % pressure of system in bar

%%%% for 1-CO2 - 2-DMAC %%%%%%%

IIc12=(aT2(1)*aT2(2))^(1/2)*(1-IIk12+IIx21*(IIk12-IIk21));

%%%% for 1-CO2 - 3-H20 %%%%%%%

IIc13=(aT2(1)*aT2(3))^(1/2)*(1-IIk13+IIx21*(IIk13-IIk31));

%%%% for 2-DMAC - 3-H20 %%%%%%%

IIc23=(aT2(2)*aT2(3))^(1/2)*(1-k23+IIx22*(k23-k32));

c2=IIx21*IIx21*aT2(1)+IIx22*IIx22*aT2(2)+IIx23*IIx23*aT2(3)+2*IIx21*II
x22*IIc12+2*IIx1*IIx3*IIc13+2*IIx2*IIx3*IIc23;
d2=IIx21*bT(1)+IIx22*bT(2)+IIx23*bT(3);


C2=c2*IIP2/(R*T2)^2;
D2=d2*IIP2/(R*T2);

IIs21=1;
IIs22=-(1-D2);
IIs23=C2-3*D2^2-2*D2;
IIs24=-(C2*D2-D2^2-D2^3);
IIpx2=[IIs21 IIs22 IIs23 IIs24];
IIZx2=roots(IIpx2)
IIv=0;
for q=1:3
    TF=isreal(IIZx2(q));
    if TF==1
        IIv=IIv+1;
        IIZvap(IIv)=IIZx2(q);
    end;
end;
IIZ2=max(IIZvap)

IIKexp2=0.08553;
IIgamma2=0.4146;
IIfi2=0.0075;
```

```
% FOR 241 BAR

IIx32=0.000275453;            % mole fraction of DMAc
IIx33=0.004;                  % mole fraction of H2O from K=0.0040
IIx31=1-IIx32-IIx33;          % mole fraction of CO2

IIP3=241; % pressure of system in bar


%%%% for 1-CO2 - 2-DMAC %%%%%%%

IIe12=(aT2(1)*aT2(2))^(1/2)*(1-IIk12+IIx31*(IIk12-IIk21));


%%%% for 1-CO2 - 3-H20 %%%%%%%

IIe13=(aT2(1)*aT2(3))^(1/2)*(1-IIk13+IIx31*(IIk13-IIk31));

%%%% for 2-DMAC - 3-H20 %%%%%%%

IIe23=(aT2(2)*aT2(3))^(1/2)*(1-k23+IIx32*(k23-k32));

e2=IIx31*IIx31*aT2(1)+IIx32*IIx32*aT2(2)+IIx33*IIx33*aT2(3)+2*IIx31*II
x32*IIe12+2*IIx31*IIx33*IIe13+2*IIx2*IIx3*IIe23;
f2=IIx31*bT(1)+IIx32*bT(2)+IIx33*bT(3);


E2=e2*IIP3/(R*T2)^2;
F2=f2*IIP3/(R*T2);

IIs31=1;
IIs32=-(1-F2);
IIs33=E2-3*F2^2-2*F2;
IIs34=-(E2*F2-F2^2-F2^3);
IIpx3=[IIs31 IIs32 IIs33 IIs34];
IIZx3=roots(IIpx3)
IIv=0;
for q=1:3
    TF=isreal(IIZx3(q));
    if TF==1
        IIv=IIv+1;
        IIZvap(v)=IIZx3(q);
    end;
end;
IIZ3=max(IIZvap)

IIKexp3=0.0977;
IIgamma3=0.4144;
```

```
IIfi3=0.011;




%%%%%%%%%%  3.   318 K ALL PRESSURES  %%%%%%%%%%%%%%%
T3=318.2;          % temperature of the system, in K

for i=1:3
    aTc(i)=0.45724*R^2*Tc(i)^2/Pc(i);
    bTc(i)=0.07780*R*Tc(i)/Pc(i);
    kappa(i)=0.37464+1.54226*om(i)-0.26992*om(i)^2;
    Tr3(i)=T3/Tc(i);
    alpha3(i)=(1+kappa(i)*(1-(Tr3(i))^0.5))^2;
    aT3(i)=aTc(i)*alpha3(i);
    bT(i)=bTc(i);
end;

% FOR 138 BAR

IIIx2=0.000255184;            % mole fraction of DMAc
IIIx3=0.004;                  % mole fraction of H2O from K=0.0040
IIIx1=1-IIIx2-IIIx3;          % mole fraction of CO2

IIIP1=138; % pressure of system in bar

%%%% for 1-CO2 - 2-DMAC %%%%%%%
IIIk12=A0(1)+A0(2)*T3;
IIIk21=A0(3)+A0(4)*T3;
IIIa12=(aT3(1)*aT3(2))^(1/2)*(1-IIIk12+IIIx1*(IIIk12-IIIk21));

%%%% for 1-CO2 - 3-H20 %%%%%%%
IIIk13=-0.4271+1.0377e-3*T3;        %from Maurer
IIIk31=-0.4516+1.9813e-3*T3;        %from Maurer
IIIa13=(aT3(1)*aT3(3))^(1/2)*(1-IIIk13+IIIx1*(IIIk13-IIIk31));

%%%% for 2-DMAC - 3-H20 %%%%%%%

IIIa23=(aT3(2)*aT3(3))^(1/2)*(1-k23+IIIx2*(k23-k32));

a3=IIIx1*IIIx1*aT3(1)+IIIx2*IIIx2*aT3(2)+IIIx3*IIIx3*aT3(3)+2*IIIx1*II
Ix2*IIIa12+2*IIIx1*IIIx3*IIIa13+2*IIIx2*IIIx3*IIIa23;
b3=IIIx1*bT(1)+IIIx2*bT(2)+IIIx3*bT(3);


A3=a3*IIIP1/(R*T3)^2;
B3=b3*IIIP1/(R*T3);
```

```
IIIs1=1;
IIIs2=-(1-B3);
IIIs3=A3-3*B3^2-2*B3;
IIIs4=-(A3*B3-B3^2-B3^3);
IIIpx=[IIIs1 IIIs2 IIIs3 IIIs4];
IIIZx=roots(IIIpx)
IIIv=0;
for q=1:3
    TF=isreal(IIIZx(q));
    if TF==1
        IIIv=IIIv+1;
        IIIZvap(IIIv)=IIIZx(q);
    end;
end;
IIIZ1=max(IIIZvap)

IIIKexp1=0.080827;
IIIgamma1=0.4148;
IIIfi1=0.014;

%%%%%%%%%%%%%%%%%% FOR 172 BAR  %%%%%%%%%%%%

IIIx22=0.000279561;          % mole fraction of DMAc
IIIx23=0.004;                % mole fraction of H2O from K=0.0040
IIIx21=1-IIIx22-IIIx23;      % mole fraction of CO2

IIIP2=172; % pressure of system in bar

%%%% for 1-CO2 - 2-DMAC %%%%%%%

IIIc12=(aT3(1)*aT3(2))^(1/2)*(1-IIIk12+IIIx21*(IIIk12-IIIk21));

%%%% for 1-CO2 - 3-H20 %%%%%%%

IIIc13=(aT3(1)*aT3(3))^(1/2)*(1-IIIk13+IIIx21*(IIIk13-IIIk31));

%%%% for 2-DMAC - 3-H20 %%%%%%%

IIIc23=(aT3(2)*aT3(3))^(1/2)*(1-k23+IIIx22*(k23-k32));

c3=IIIx21*IIIx21*aT3(1)+IIIx22*IIIx22*aT3(2)+IIIx23*IIIx23*aT3(3)+2*II
Ix21*IIIx22*IIIc12+2*IIIx1*IIIx3*IIIc13+2*IIIx2*IIIx3*IIIc23;
d3=IIIx21*bT(1)+IIIx22*bT(2)+IIIx23*bT(3);


C3=c3*IIIP2/(R*T3)^2;
D3=d3*IIIP2/(R*T3);
```

```
IIIs21=1;
IIIs22=-(1-D3);
IIIs23=C3-3*D3^2-2*D3;
IIIs24=-(C3*D3-D3^2-D3^3);
IIIpx2=[IIIs21 IIIs22 IIIs23 IIIs24];
IIIZx2=roots(IIIpx2)
IIIv=0;
for q=1:3
    TF=isreal(IIIZx2(q));
    if TF==1
        IIIv=IIIv+1;
        IIIZvap(IIIv)=IIIZx2(q);
    end;
end;
IIIZ2=max(IIIZvap)

IIIKexp2=0.094081;
IIIgamma2=0.4145;
IIIfi2=0.0158;

%%%%%%%%%%%%%%%%%%% FOR 241 BAR %%%%%%%%%%%%%%

IIIx32=0.000320736;          % mole fraction of DMAc
IIIx33=0.004;                % mole fraction of H2O from K=0.0040
IIIx31=1-IIIx32-IIIx33;      % mole fraction of CO2

IIIP3=241; % pressure of system in bar


%%%% for 1-CO2 - 2-DMAC %%%%%%%

IIIe12=(aT3(1)*aT3(2))^(1/2)*(1-IIIk12+IIIx31*(IIIk12-IIIk21));

%%%% for 1-CO2 - 3-H20 %%%%%%%

IIIe13=(aT3(1)*aT3(3))^(1/2)*(1-IIIk13+IIIx31*(IIIk13-IIIk31));

%%%% for 2-DMAC - 3-H20 %%%%%%%

IIIe23=(aT3(2)*aT3(3))^(1/2)*(1-k23+IIIx32*(k23-k32));

e3=IIIx31*IIIx31*aT3(1)+IIIx32*IIIx32*aT3(2)+IIIx33*IIIx33*aT3(3)+2*II
Ix31*IIIx32*IIIe12+2*IIIx31*IIIx33*IIIe13+2*IIIx2*IIIx3*IIIe23;
f3=IIIx31*bT(1)+IIIx32*bT(2)+IIIx33*bT(3);


E3=e3*IIIP3/(R*T3)^2;
F3=f3*IIIP3/(R*T3);
```

```
IIIs31=1;
IIIs32=-(1-F3);
IIIs33=E3-3*F3^2-2*F3;
IIIs34=-(E3*F3-F3^2-F3^3);
IIIpx3=[IIIs31 IIIs32 IIIs33 IIIs34];
IIIZx3=roots(IIIpx3)
IIIv=0;
for q=1:3
    TF=isreal(IIIZx3(q));
    if TF==1
        IIIv=IIIv+1;
        IIIZvap(v)=IIIZx3(q);
    end;
end;
IIIZ3=max(IIIZvap)

IIIKexp3=0.119663;
IIIgamma3=0.4142;
IIIfi3=0.0201;

%%%%%%%%%%%% 4. FOR ALL 328 K
T4=328.2; % temp. of system, in K
for i=1:3
    aTc(i)=0.45724*R^2*Tc(i)^2/Pc(i);
    bTc(i)=0.07780*R*Tc(i)/Pc(i);
    kappa(i)=0.37464+1.54226*om(i)-0.26992*om(i)^2;
    Tr4(i)=T4/Tc(i);
    alpha4(i)=(1+kappa(i)*(1-(Tr4(i))^0.5))^2;
    aT4(i)=aTc(i)*alpha4(i);
    bT(i)=bTc(i);
end;

% FOR 172 BAR
IVx2=0.000308861;            % mole fraction of DMAc
IVx3=0.004;                  % mole fraction of H2O from K=0.0040
IVx1=1-IVx2-IVx3;            % mole fraction of CO2

IVP1=172; % pressure of system in bar

%%%% for 1-CO2 - 2-DMAC %%%%%%%
IVk12=A0(1)+A0(2)*T4;
IVk21=A0(3)+A0(4)*T4;
IVa12=(aT4(1)*aT4(2))^(1/2)*(1-IVk12+IVx1*(IVk12-IVk21));

%%%% for 1-CO2 - 3-H20 %%%%%%%
IVk13=-0.4271+1.0377e-3*T4;         %from Maurer
IVk31=-0.4516+1.9813e-3*T4;         %from Maurer
IVa13=(aT4(1)*aT4(3))^(1/2)*(1-IVk13+IVx1*(IVk13-IVk31));

%%%% for 2-DMAC - 3-H20 %%%%%%%
```

```
IVa23=(aT4(2)*aT4(3))^(1/2)*(1-k23+IVx2*(k23-k32));

a4=IVx1*IVx1*aT4(1)+IVx2*IVx2*aT4(2)+IVx3*IVx3*aT4(3)+2*IVx1*IVx2*IVa1
2+2*IVx1*IVx3*IVa13+2*IVx2*IVx3*IVa23;
b4=IVx1*bT(1)+IVx2*bT(2)+IVx3*bT(3);

A4=a4*IVP1/(R*T4)^2;
B4=b4*IVP1/(R*T4);

IVs1=1;
IVs2=-(1-B4);
IVs3=A4-3*B4^2-2*B4;
IVs4=-(A4*B4-B4^2-B4^3);
IVpx=[IVs1 IVs2 IVs3 IVs4];
IVZx=roots(IVpx)
IVv=0;
for q=1:3
    TF=isreal(IVZx(q));
    if TF==1
        IVv=IVv+1;
        IVZvap(IVv)=IVZx(q);
    end;
end;
IVZ1=max(IVZvap)

IVKexp1=0.104234;
IVgamma1=0.4145;
IVfi1=0.0237;


%%%%%%%%%%%% FOR 193 BAR %%%%%%%%%

IVx22=0.000344118;            % mole fraction of DMAc
IVx23=0.004;                  % mole fraction of H2O from K=0.0040
IVx21=1-IVx22-IVx23;          % mole fraction of CO2

IVP2=193; % pressure of system in bar( 1200,2000,3500psi)

%%%% for 1-CO2 - 2-DMAC %%%%%%%

IVc12=(aT4(1)*aT4(2))^(1/2)*(1-IVk12+IVx21*(IVk12-IVk21));

%%%% for 1-CO2 - 3-H20 %%%%%%%

IVc13=(aT4(1)*aT4(3))^(1/2)*(1-IVk13+IVx21*(IVk13-IVk31));

%%%% for 2-DMAC - 3-H20 %%%%%%%

IVc23=(aT4(2)*aT4(3))^(1/2)*(1-k23+IVx22*(k23-k32));
```

```
c4=IVx21*IVx21*aT4(1)+IVx22*IVx22*aT4(2)+IVx23*IVx23*aT4(3)+2*IVx21*IV
x22*IVc12+2*IVx1*IVx3*IVc13+2*IVx2*IVx3*IVc23;
d4=IVx21*bT(1)+IVx22*bT(2)+IVx23*bT(3);


C4=c4*IVP2/(R*T4)^2;
D4=d4*IVP2/(R*T4);

IVs21=1;
IVs22=-(1-D4);
IVs23=C4-3*D4^2-2*D4;
IVs24=-(C4*D4-D4^2-D4^3);
IVpx2=[IVs21 IVs22 IVs23 IVs24];
IVZx2=roots(IVpx2)
IVv=0;
for q=1:3
    TF=isreal(IVZx2(q));
    if TF==1
        IVv=IVv+1;
        IVZvap(IVv)=IVZx2(q);
    end;
end;
IVZ2=max(IVZvap)

IVKexp2=0.12444;
IVgamma2=0.4143;
IVfi2=0.0286;

% FOR 241 BAR

IVx32=0.000375104;            % mole fraction of DMAc
IVx33=0.004;                  % mole fraction of H2O from K=0.0040
IVx31=1-IVx32-IVx33;          % mole fraction of CO2

IVP3=241; % pressure of system in bar( 1200,2000,3500psi)


%%%% for 1-CO2 - 2-DMAC %%%%%%%

IVe12=(aT4(1)*aT4(2))^(1/2)*(1-IVk12+IVx31*(IVk12-IVk21));


%%%% for 1-CO2 - 3-H20 %%%%%%%

IVe13=(aT4(1)*aT4(3))^(1/2)*(1-IVk13+IVx31*(IVk13-IVk31));

%%%% for 2-DMAC - 3-H20 %%%%%%%
```

```
IVe23=(aT4(2)*aT4(3))^(1/2)*(1-k23+IVx32*(k23-k32));

e4=IVx31*IVx31*aT4(1)+IVx32*IVx32*aT4(2)+IVx33*IVx33*aT2(3)+2*IVx31*IV
x32*IVe12+2*IVx31*IVx33*IVe13+2*IVx2*IVx3*IVe23;
f4=IVx31*bT(1)+IVx32*bT(2)+IVx33*bT(3);


E4=e4*IVP3/(R*T4)^2;
F4=f4*IVP3/(R*T4);

IVs31=1;
IVs32=-(1-F4);
IVs33=E4-3*F4^2-2*F4;
IVs34=-(E4*F4-F4^2-F4^3);
IVpx3=[IVs31 IVs32 IVs33 IVs34];
IVZx3=roots(IVpx3)
IVv=0;
for q=1:3
    TF=isreal(IVZx3(q));
    if TF==1
        IVv=IVv+1;
        IVZvap(v)=IVZx3(q);
    end;
end;
IVZ3=max(IVZvap)

IVKexp3=0.14835;
IVgamma3=0.4140;
IVfi3=0.0337;



F = [(Kexp1-gamma1*fi1/(P1*(exp(bT(2)/b1*(Z1-1)-log(Z1-B1)-
A1/(2*2^0.5*B1)*(2*(x1*a12+x2*aT1(2)+x3*a23)/a1-
bT(2)/b1)*log((Z1+2.414*B1)/(Z1-0.414*B1))))))^2+(Kexp2-
gamma2*fi2/(P2*(exp(bT(2)/d1*(Z2-1)-log(Z2-D1)-
C1/(2*2^0.5*D1)*(2*(x21*c12+x22*aT1(2)+x23*c23)/c1-
bT(2)/d1)*log((Z2+2.414*D1)/(Z2-0.414*D1))))))^2+(Kexp3-
gamma3*fi3/(P3*(exp(bT(2)/f1*(Z3-1)-log(Z3-F1)-
E1/(2*2^0.5*F1)*(2*(x31*e12+x32*aT1(2)+x33*e23)/e1-
bT(2)/f1)*log((Z3+2.414*F1)/(Z3-0.414*F1))))))^2;
    (IIKexp1-IIgamma1*IIfi1/(IIP1*(exp(bT(2)/b2*(IIZ1-1)-log(IIZ1-B2)-
A2/(2*2^0.5*B2)*(2*(IIx1*IIa12+IIx2*aT2(2)+IIx3*IIa23)/a2-
bT(2)/b2)*log((IIZ1+2.414*B2)/(IIZ1-0.414*B2))))))^2+(IIKexp2-
IIgamma2*IIfi2/(IIP2*(exp(bT(2)/d2*(IIZ2-1)-log(IIZ2-D2)-
C2/(2*2^0.5*D2)*(2*(IIx21*IIc12+IIx22*aT2(2)+IIx23*IIc23)/c2-
bT(2)/d2)*log((IIZ2+2.414*D2)/(IIZ2-0.414*D2))))))^2+(IIKexp3-
IIgamma3*IIfi3/(IIP3*(exp(bT(2)/f2*(IIZ3-1)-log(IIZ3-F2)-
E2/(2*2^0.5*F2)*(2*(IIx31*IIe12+IIx32*aT2(2)+IIx33*IIe23)/e2-
bT(2)/f2)*log((IIZ3+2.414*F2)/(IIZ3-0.414*F2))))))^2;
```

```
    (IIIKexp1-IIIgamma1*IIIfi1/(IIIP1*(exp(bT(2)/b3*(IIIZ1-1)-
log(IIIZ1-B3)-
A3/(2*2^0.5*B3)*(2*(IIIx1*IIIa12+IIIx2*aT3(2)+IIIx3*IIIa23)/a3-
bT(2)/b3)*log((IIIZ1+2.414*B3)/(IIIZ1-0.414*B3))))))^2+(IIIKexp2-
IIIgamma2*IIIfi2/(IIIP2*(exp(bT(2)/d3*(IIIZ2-1)-log(IIIZ2-D3)-
C3/(2*2^0.5*D3)*(2*(IIIx21*IIIc12+IIIx22*aT3(2)+IIIx23*IIIc23)/c3-
bT(2)/d3)*log((IIIZ2+2.414*D3)/(IIIZ2-0.414*D3))))))^2+(IIIKexp3-
IIIgamma3*IIIfi3/(IIIP3*(exp(bT(2)/f3*(IIIZ3-1)-log(IIIZ3-F3)-
E3/(2*2^0.5*F3)*(2*(IIIx31*IIIe12+IIIx32*aT3(2)+IIIx33*IIIe23)/e3-
bT(2)/f3)*log((IIIZ3+2.414*F3)/(IIIZ3-0.414*F3))))))^2;
    (IVKexp1-IVgamma1*IVfi1/(IVP1*(exp(bT(2)/b4*(IVZ1-1)-log(IVZ1-B4)-
A4/(2*2^0.5*B4)*(2*(IVx1*IVa12+IVx2*aT4(2)+IVx3*IVa23)/a4-
bT(2)/b4)*log((IVZ1+2.414*B4)/(IVZ1-0.414*B4))))))^2+(IVKexp2-
IVgamma2*IVfi2/(IVP2*(exp(bT(2)/d4*(IVZ2-1)-log(IVZ2-D4)-
C4/(2*2^0.5*D4)*(2*(IVx21*IVc12+IVx22*aT4(2)+IVx23*IVc23)/c4-
bT(2)/d4)*log((IVZ2+2.414*D4)/(IVZ2-0.414*D4))))))^2+(IVKexp3-
IVgamma3*IVfi3/(IVP3*(exp(bT(2)/f4*(IVZ3-1)-log(IVZ3-F4)-
E4/(2*2^0.5*F4)*(2*(IVx31*IVe12+IVx32*aT4(2)+IVx33*IVe23)/e4-
bT(2)/f4)*log((IVZ3+2.414*F4)/(IVZ3-0.414*F4))))))^2];
```

APPENDIX 2

BUBBLE POINT PRESSURE CALCULATIONS

MATLAB Programme

```
clear all;
close all;
clc;

global aij bij delij dijcalc n0 aT bT yexp P R T x ax Ax bx Bx ay Ay
by By Zl li ynew Zv y TKixi K fval exitflag y0 yguess output PhiL PhiV
Perrtot Pcalc Pexp ycalc Zcalc Zvcalc exf fv PhiL PhiV P0exp X

% Component properties
% 1-CO2 2-DMAC
Tc=[304.19
    658];          % in K
Pc=[73.82
    40.3];         % in bar
om=[0.23
    0.3635];       % acentric factor at Tr = 0.7;

gdata=[0.05274
    0.2289
    0.3918
    0.6173
    0.7604
    0.8524];


xexp=ones(size(gdata))-gdata;


for i=1:size(xexp)
    X(i,1)=xexp(i);
    X(i,2)=1-xexp(i);
end;
```

```
P0exp=[61
    61
    55
    41
    21
    15];



Pexp=[62.85714286
    59.86394558
    47.61904762
    29.25170068
    17.00680272
    10.40816327];


yexp=0.99*ones(size(X,1),1);


T=298.2;          % temperature of the system, in K
R=83.1447;        % gas constant, cm3*bar/(mol*K)

for i=1:2
    aTc(i)=0.45724*R^2*Tc(i)^2/Pc(i);
    bTc(i)=0.07780*R*Tc(i)/Pc(i);
    kappa(i)=0.37464+1.54226*om(i)-0.26992*om(i)^2;
    Tr(i)=T/Tc(i);
    alpha(i)=(1+kappa(i)*(1-(Tr(i))^0.5))^2;
    aT(i)=aTc(i)*alpha(i);
    bT(i)=bTc(i);
end;


Perrtot=1;
n=0;
binij=[-0.0712
    0.0043];

%%
delij=[0 binij(1)
    binij(2) 0];
% nij=[0 binij(2)
%     binij(2) 0];
for i=1:2
    for j=1:2
        aij(i,j)=aT(i)^0.5*aT(j)^0.5;
    end;
end;
```

```
l=0;

for l=1:size(X,1)
    P=0;
    y=0;
    ynew=0;
    Zv=0;
    Zl=0;
    x=(X(l,:))';
    P0=P0exp(l);

    ax=0;
    bx=0;
    for i=1:2
        for j=1:2
            ax=ax+x(i)*x(j)*aij(i,j)*(1-delij(i,j)+(delij(i,j)-
delij(j,i))*x(i));
        end;
        bx=bx+x(i)*bT(i);
    end;
    TKixi=0;
    y0=yexp(l);
    [P,fval,exitflag]=fsolve(@runicinYeni,P0);
    if P==P0
        P01=P0-5;
        P02=P0+5;
        [P,fval,exitflag]=fminbnd(@runicinYeni,P01,P02);
    end;
    Pcalc(l)=P;
    ycalc(l)=y;
    Zlcalc(l)=Zl;
    Zvcalc(l)=Zv;
    exf(l)=exitflag;
    fv(l)=fval;
    PhiL(l)=PhiL(1);
    PhiV(l)=PhiV(1);
end;
Perrtot=0;
for m=1:size(X,1)
    Perrtot=Perrtot+abs(Pcalc(m)-Pexp(m))/Pexp(m);
end;
s=(Perrtot)^2;
n0=n0+1;

ADDP=0;
ADDy=0;
for l=1:size(X,1)
    ADDP=ADDP+abs(Pexp(l)-Pcalc(l))/Pexp(l);
    ADDy=ADDy+abs(yexp(l)-ycalc(l))/yexp(l);
end;
ADDP=ADDP/size(X,1)*100
ADDy=ADDy/size(X,1)*100
```

```
for l=1:size(X,1)
    if exf(l)==1 && Pcalc(l)~=P0exp(l) && mod(Pcalc(l),1)~=0
        disp('OK!');
    else
        disp('Not OK!');
    end;
end;
```

APPENDIX 3

UV / VIS SPECTROPHOTOMETER ANALYSIS

Calibration Curves

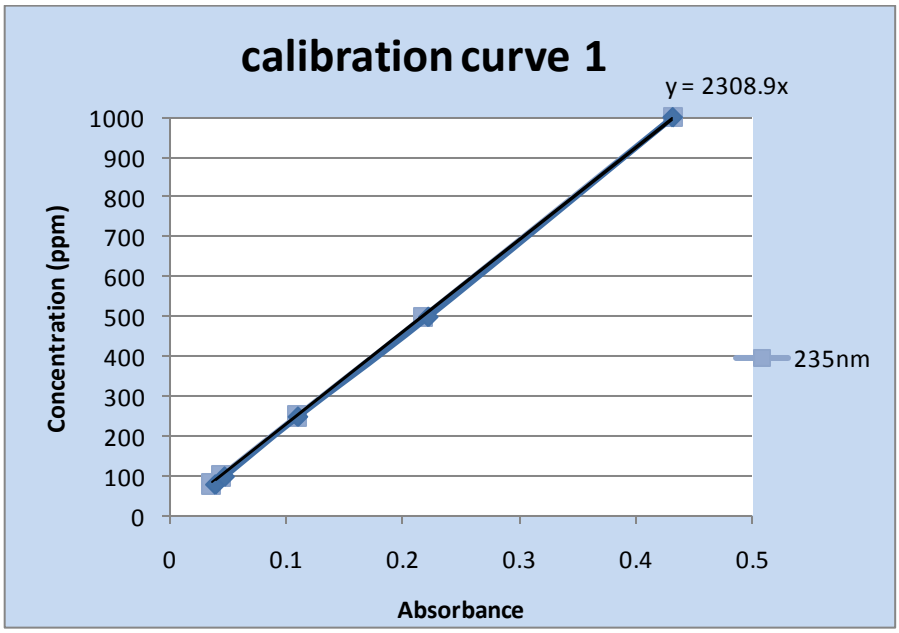

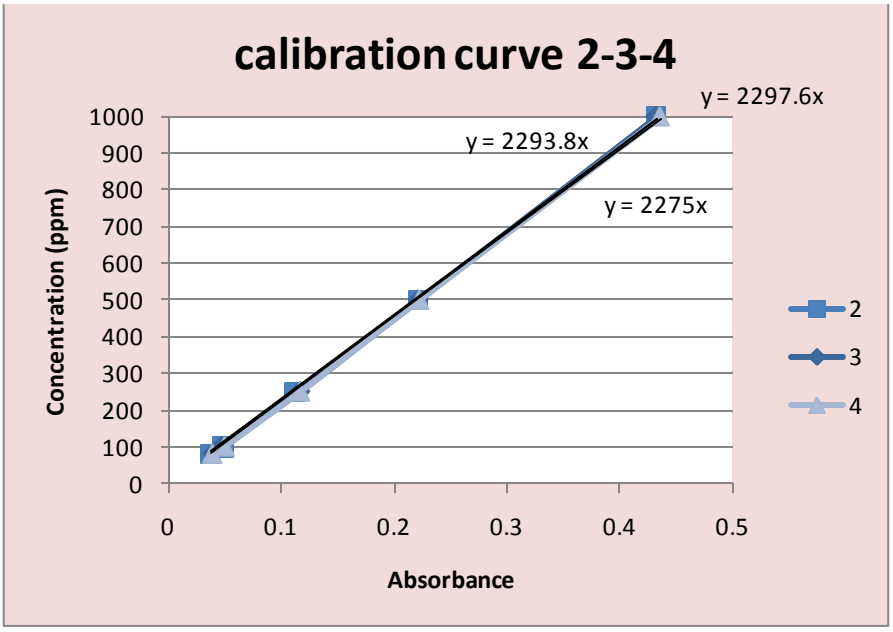

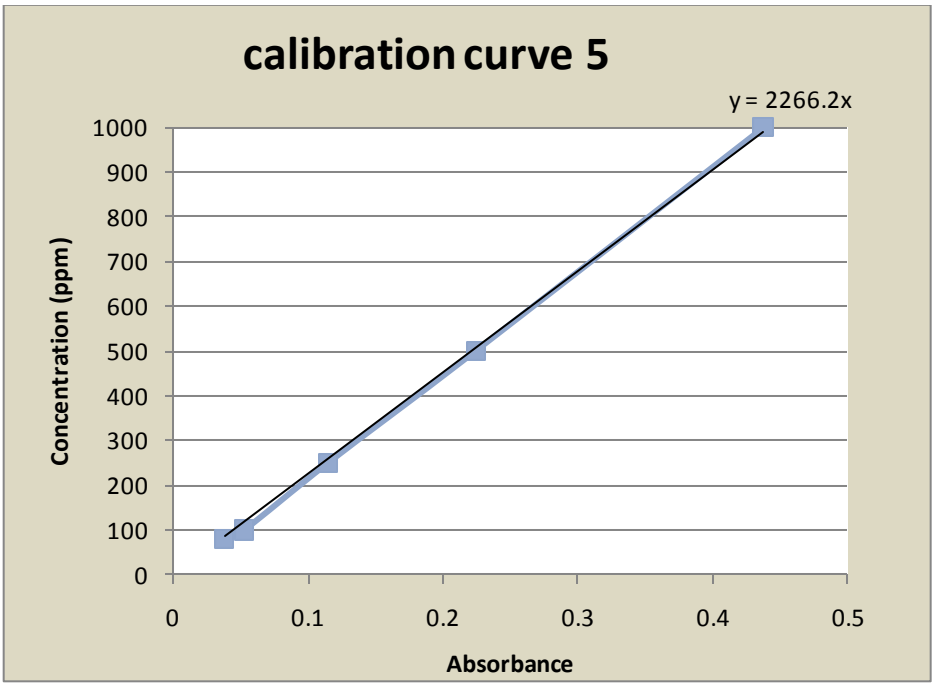
calibration curve 5
y = 2266.2x
Concentration (ppm)
1000
900
800
700
600
500
400
300
200
100
0
0
0.1
0.2
0.3
0.4
0.5
Absorbance

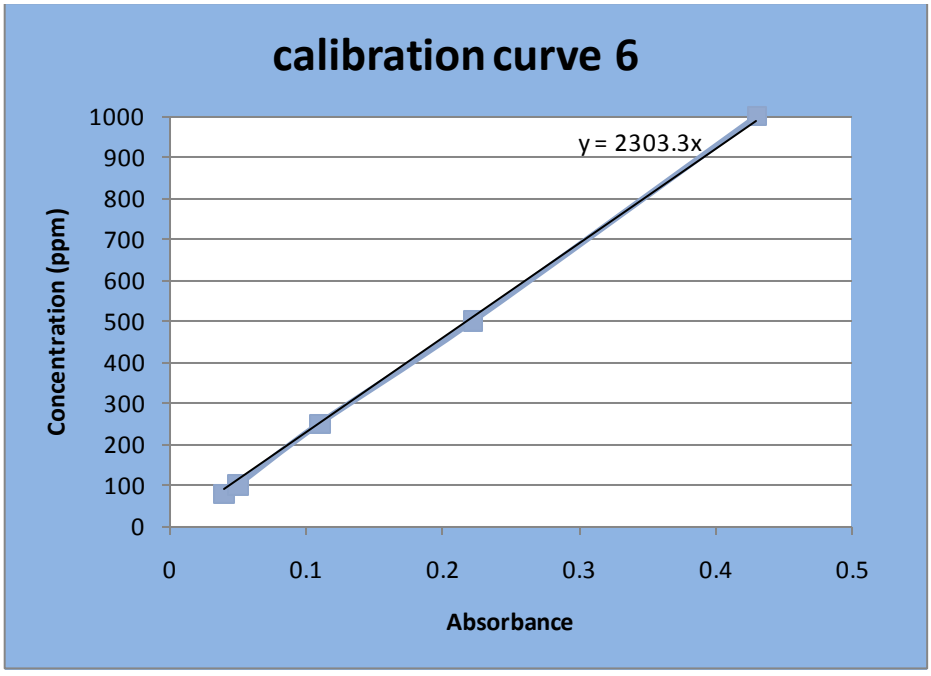
calibration curve 6
y = 2303.3x
Concentration (ppm)
1000
900
800
700
600
500
400
300
200
100
0
0
0.1
0.2
0.3
0.4
0.5
Absorbance

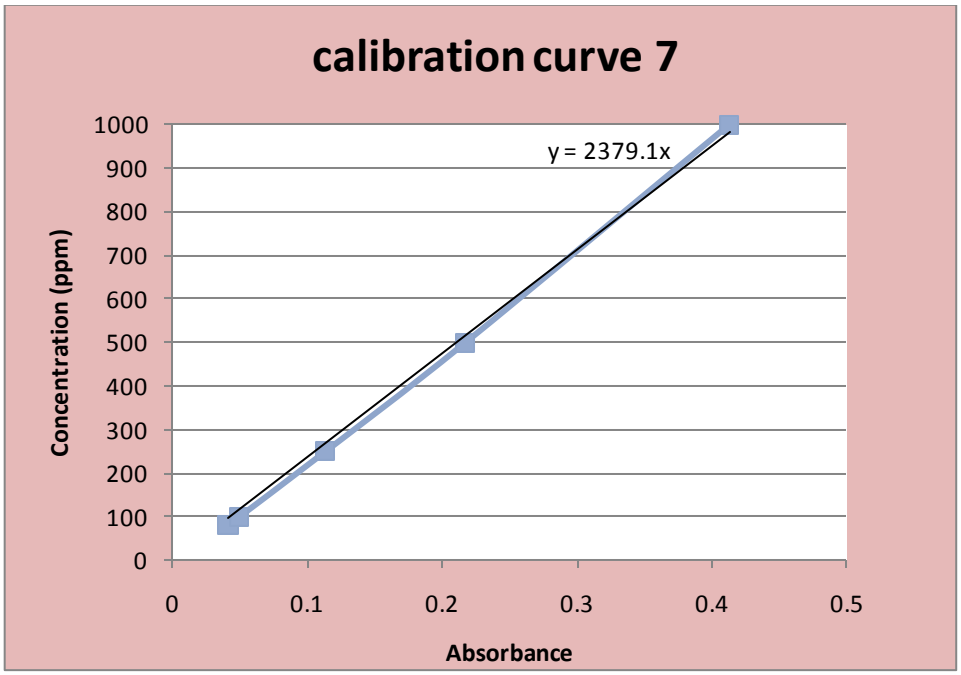
calibration curve 7
y = 2379.1x
Concentration (ppm)
1000
900
800
700
600
500
400
300
200
100
0
0
0.1
0.2
0.3
0.4
0.5
Absorbance

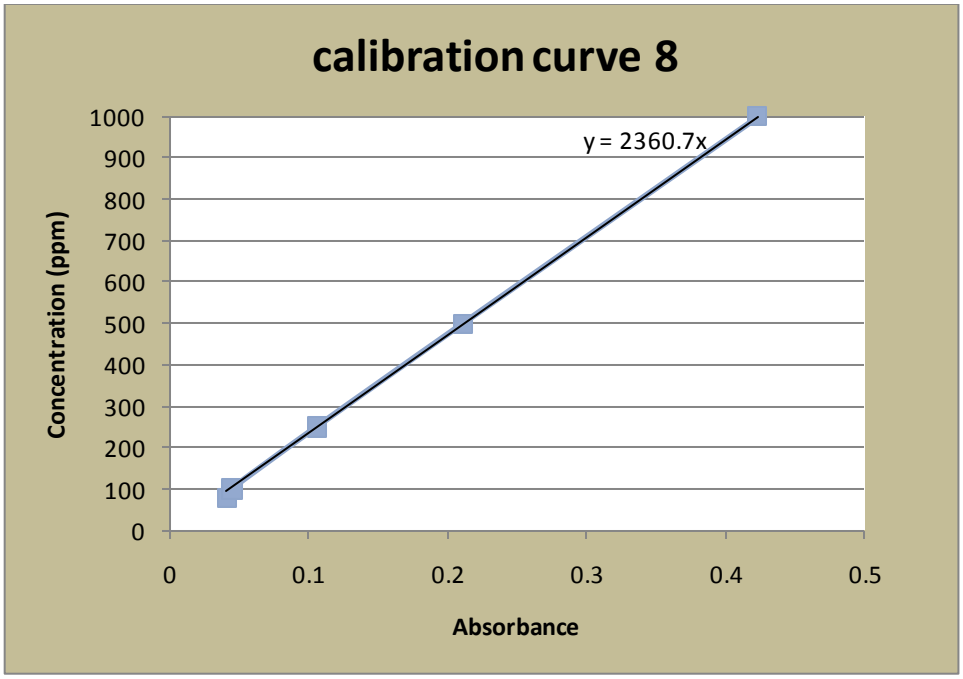
calibration curve 8
y = 2360.7x
Concentration (ppm)
1000
900
800
700
600
500
400
300
200
100
0
0
0.1
0.2
0.3
0.4
0.5
Absorbance

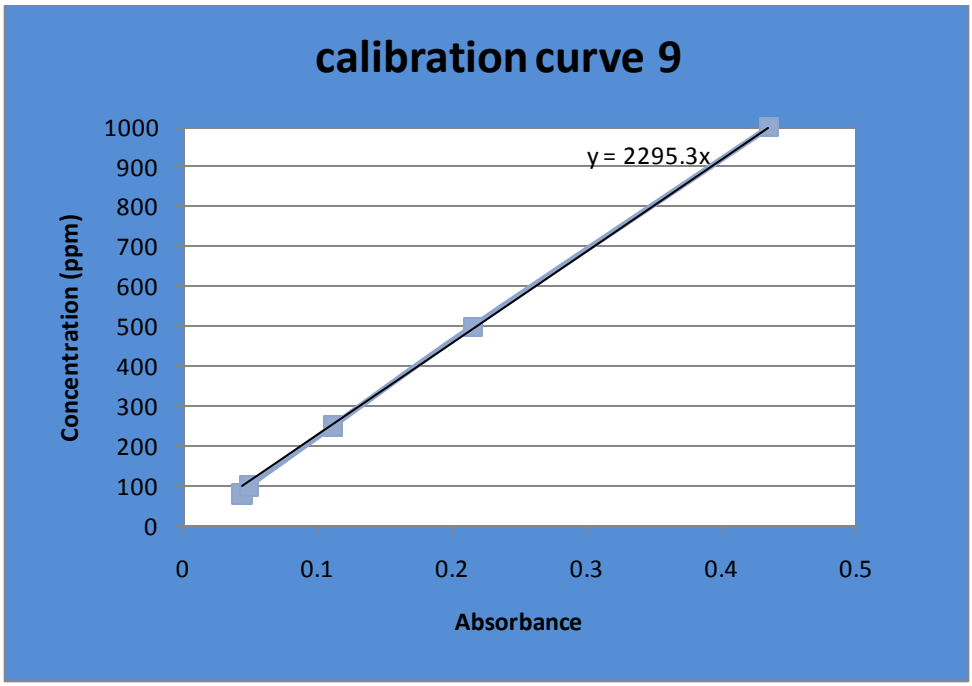
calibration curve 9
y = 2295.3x
Concentration (ppm)
1000
900
800
700
600
500
400
300
200
100
0
0
0.1
0.2
0.3
0.4
0.5
Absorbance

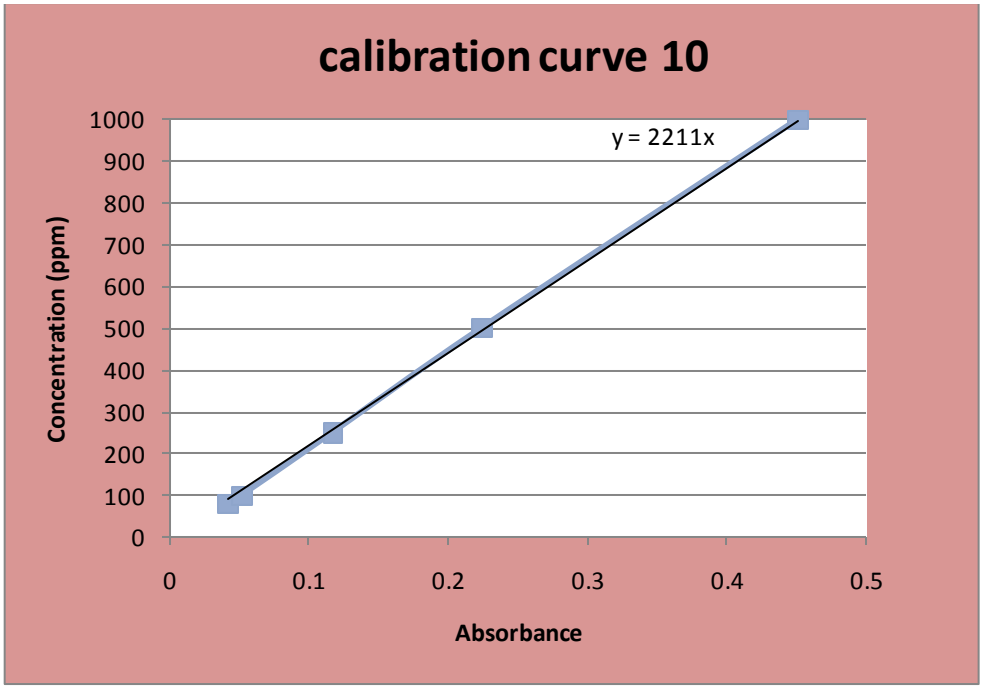
calibration curve 10
y = 2211x
Concentration (ppm)
1000
900
800
700
600
500
400
300
200
100
0
0
0.1
0.2
0.3
0.4
0.5
Absorbance

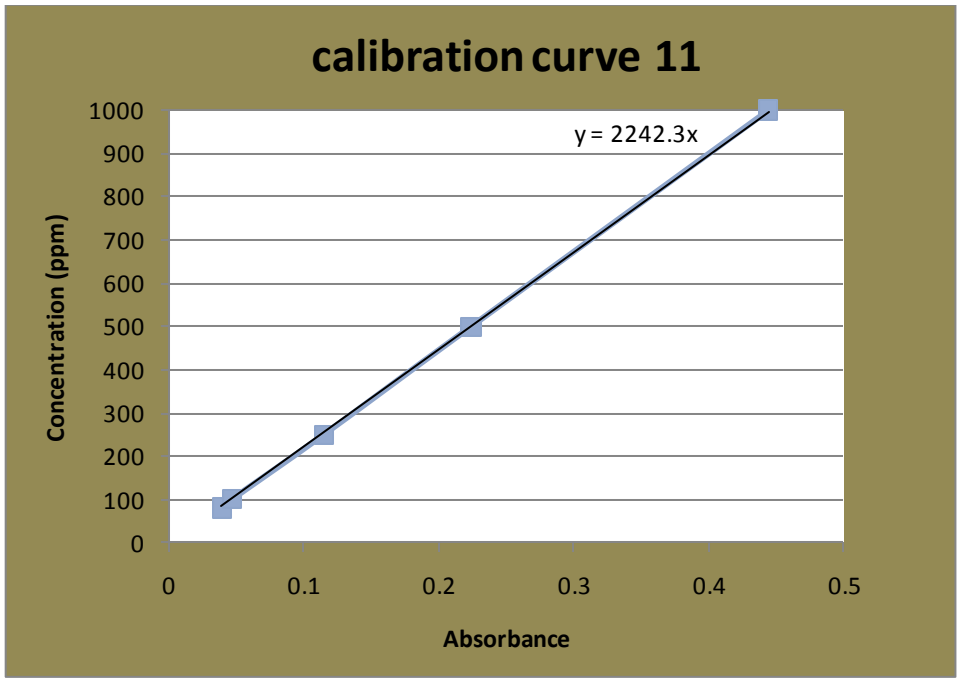
calibration curve 11
y = 2242.3x
Concentration (ppm)
1000
900
800
700
600
500
400
300
200
100
0
0
0.1
0.2
0.3
0.4
0.5
Absorbance

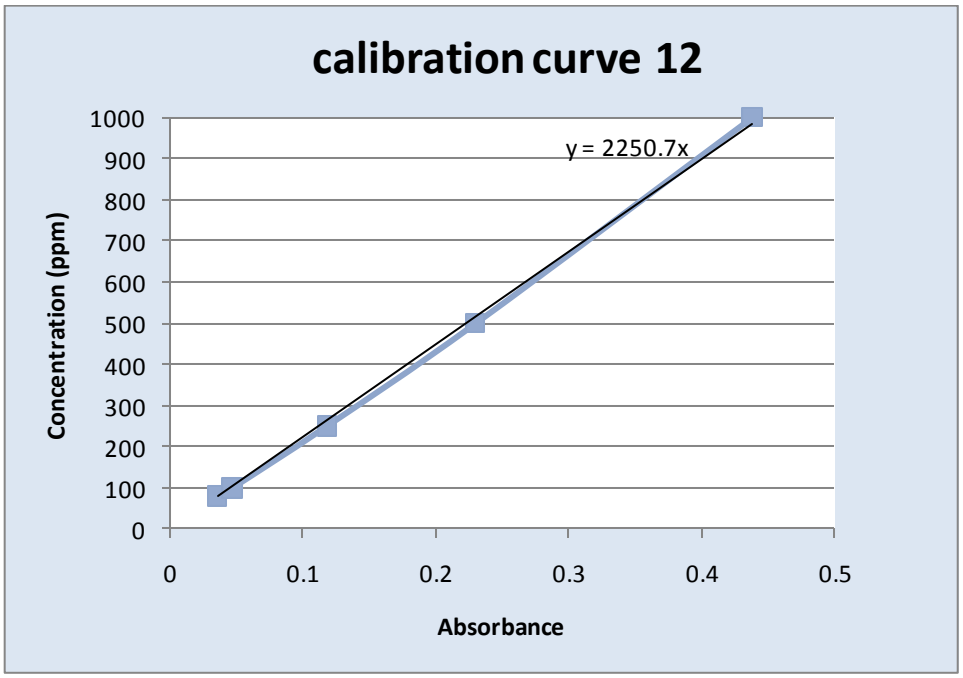
calibration curve 12
y = 2250.7x
Concentration (ppm)
1000
900
800
700
600
500
400
300
200
100
0
0
0.1
0.2
0.3
0.4
0.5
Absorbance

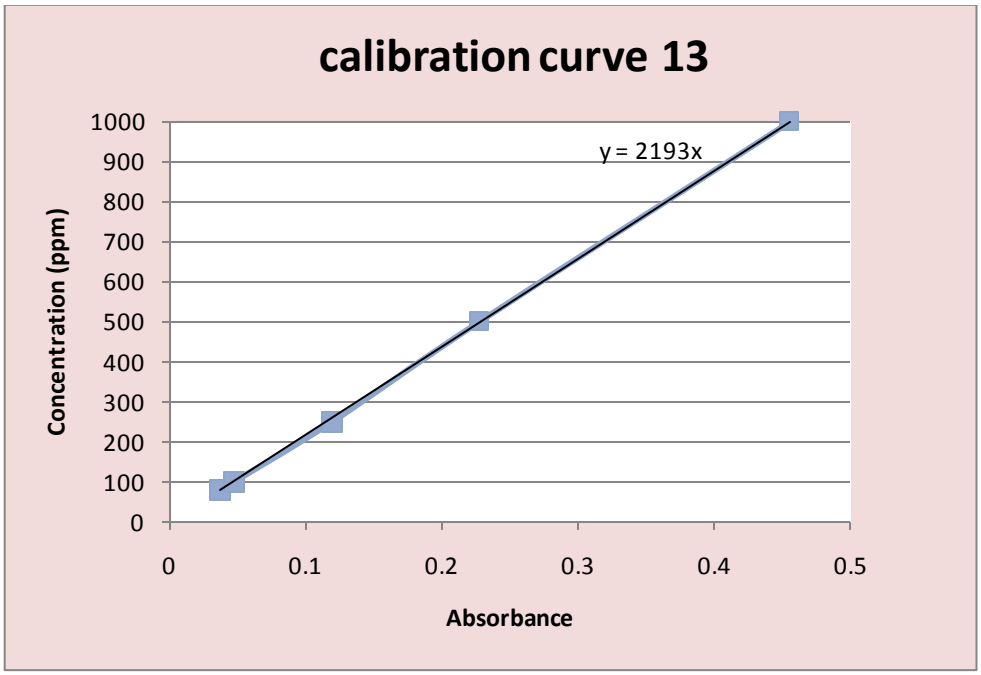
calibration curve 13
y = 2193x
Concentration (ppm)
1000
900
800
700
600
500
400
300
200
100
0
0
0.1
0.2
0.3
0.4
0.5
Absorbance

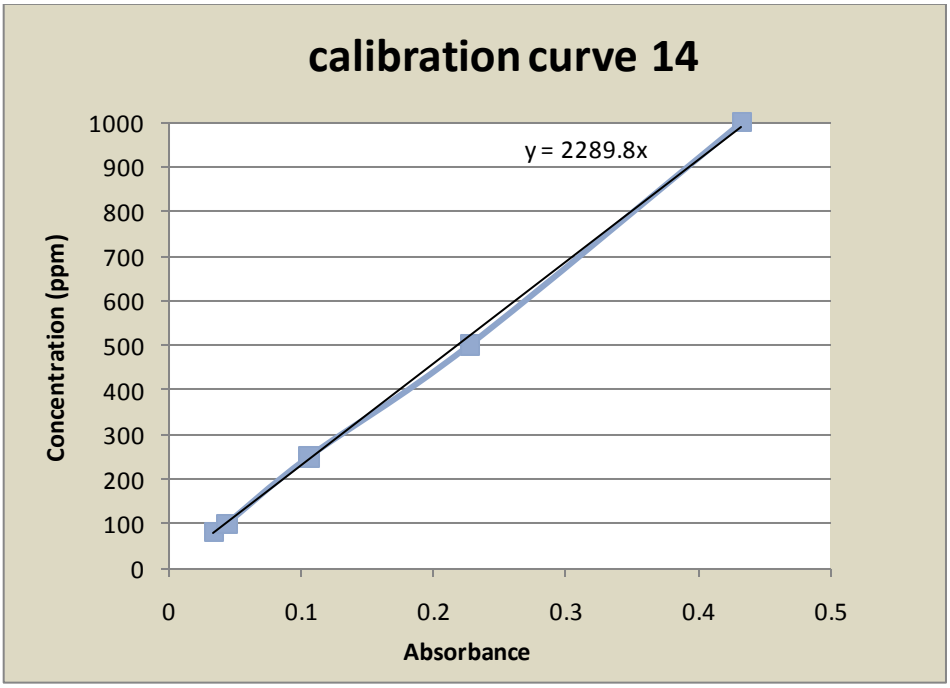
calibration curve 14
y = 2289.8x
Concentration (ppm)
1000
900
800
700
600
500
400
300
200
100
0
0
0.1
0.2
0.3
0.4
0.5
Absorbance

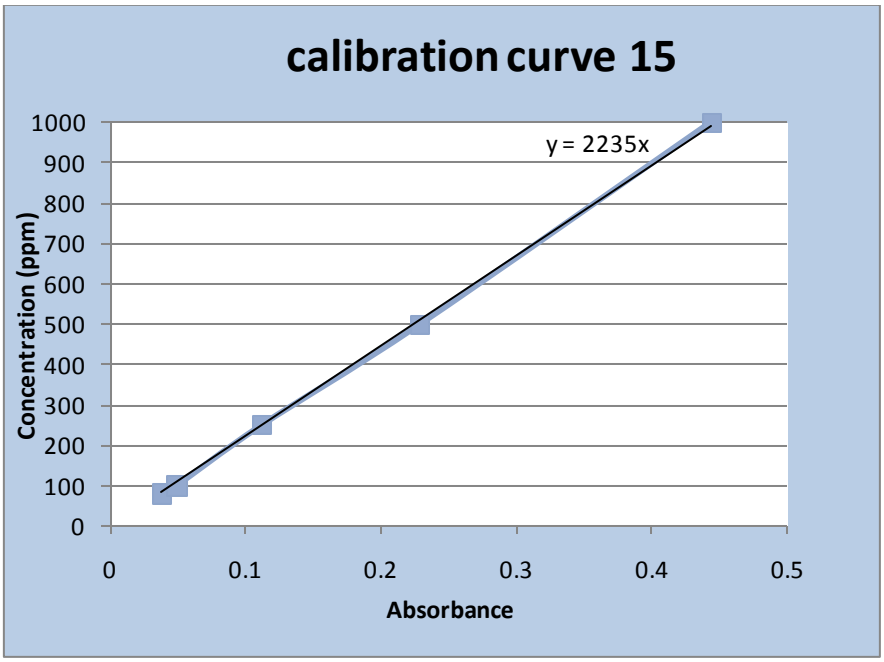
calibration curve 15
y = 2235x
Concentration (ppm)
1000
900
800
700
600
500
400
300
200
100
0
0
0.1
0.2
0.3
0.4
0.5
Absorbance

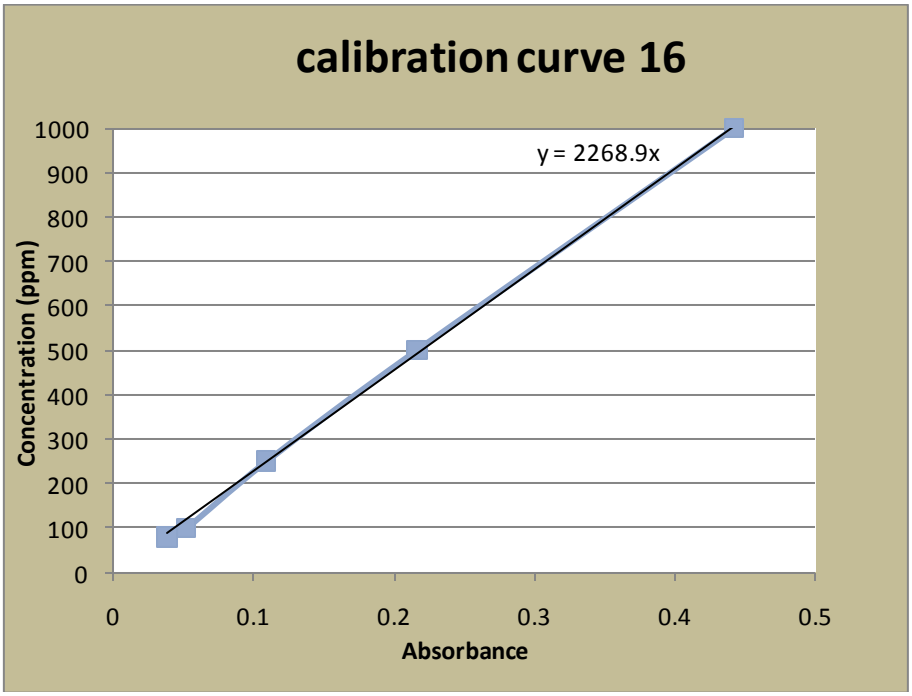
calibration curve 16
y = 2268.9x
Concentration (ppm)
1000
900
800
700
600
500
400
300
200
100
0
0
0.1
0.2
0.3
0.4
0.5
Absorbance

BIBLIOGRAPHY

[1] K. Brudi, N. Dahmen, H. Schmieder, Partition coefficient of organic substances in two-phase mixtures of water and carbon dioxide at pressures from 8 to 30 MPa and at temperatures 313 to 333 K, J. Supercrit. Fluids 9 (1996) 146 – 151

[2] A. Akgerman, B.D. Carter, Equilibrium partitioning of 2,4-dicholorophenol between water and near-critical and supercritical carbon dioxide, J. Chem. Eng. Data 39 (1994) 510 – 512.

[3] M. Budich, G. Brunner, Supercritical fluid extraction of ethanol from aqueous solutions, J. Supercrit. Fluids 25 (2003) 45 – 55

[4] M. McHugh, V. Krukonis, Supercritical Fluid Extraction: Principles and Practice, 2nd edition, (1994)

[5] A. Bamberger, G. Sieder, G. Maurer, High-pressure (vapor + liquid) equilibrium in binary mixtures of (carbon dioxide + water or acetic acid) at temperatures from 313 to 353 K, J. Supercrit. Fluids 17 (2000) 97 – 110

[6] M.T. Timko, B.F. Nicholson, J.I. Steinfeld, K. A. Smith, J.W. Tester, Partition coefficients of organic solutes between supercritical carbon dioxide and water: experimental measurements and empirical correlations, J. Chem. Eng. Data 49 (2004) 768 – 778

[7] R.K. Roop, A. Akgerman, Entrainer effect for supercritical extraction of phenol from water, Ind. Eng. Chem. Res. 28 (1989) 1542

[8] S.-D. Yeo, A. Akgerman, Supercritical extraction of organic mixtures from aqueous solutions, AIChE J. 36 (1990) 1743.

[9] D. Ghonasgi, S. Gupta, K.M. Dooley, F.C. Knopf, Supercritical CO_2 extraction of organic contaminants from aqueous streams, AIChE J. 37 (1991) 944

[10] T. Sako, T. Sugeta, N. Nakazawa, K. Otake, M. Sato, K. Ishihara, M. Kato, High pressure vapor-liquid and vapor-liquid-liquid equilibria for systems containing supercritical carbon dioxide, water and furfural, Fluid Phase Equilibria 108 (1995) 293 – 303.

[11] S. G. Kazarian, Polymer Processing with Supercritical Fluids, Polymer Science, 42, (2000), 78–101

[12] F. Cansell , C. Aymonier, A. Loppinet-Serani, Review on materials science and supercritical fluids, Current Opinion in Solid State and Materials Science, 7, (2003), 331–340.

[13] C. Erkey, Supercritical carbon dioxide extraction of metals from aqueous solutions: a review, Journal of Supercritical Fluids, 17, (2000), 259-287

[14] M. Mukhopadhyay, Natural extracts using supercritical carbon dioxide, CRC Press, LLC; 2000

[15] E.J. Beckman, Supercritical and near – critical CO_2 in green chemical synthesis and processing, J. Supercrit. Fluids 28 (2004) 121 – 191.

[16] J. F. Liu, H. J. Yang, W. Wang, Z. Li, Solubilities of amide compounds in supercritical carbon dioxide, 53, (2008), 2189 – 2192.

[17] M. Bernauer, V. Dohnal, Temperature dependence of air - water partitioning of N-Methylated (C1 and C2) fatty acid amides, J. Chem. Eng. Data 53 (2008) 2622–2631.

[18] G. Brunner, In chemical synthesis using supercritical fluids, Jessop, P., Leitner, W., Eds.; Wiley-VCH: New York, NY (1999) 88 – 107.

[19] J. L. Leazer, A. Houck, S. Gant, W. Leonard, C. J. Welch, Removal of common organic solvents from aqueous waste streams via supercritical CO_2 extraction: A potential green approach to sustainable waste management in the pharmaceutical industry, Environ. Sci. Technol. 43 (2009) 2018–2021.

[20] J. L. Hedrick, L. T. Taylor, Supercritical fluid extraction strategies of aqueous based matrices. J. High Res Chromatogr. 13 (1990) 312–316.

[21] J. L. Hedrick, L. T. Taylor, Direct supercritical fluid extraction of nitrogenous bases from aqueous solution. J. High Res. Chromatogr. 15 (1992) 151–154.

[22] R. K. Roop, A. Akgerman, E. K. Stevens, Supercritical extraction of creosote from water with toxicological validation., J. Supercrit. Fluids 1 (1988) 31–36.

[23] H.F. Hardman, Dehydration of water soluble monomers with liquid carbon dioxide, U.S. Patent 4,253,948 (1981).

[24] E.J. Shimshick, Removal of organic acids from dilute aqueous solutions of salts of organic acids by supercritical fluids, U. S. Patent 4,250,331 (1981).

[25] V.S. Bhise, Cobalt carbonyl catalyzed olefin hydroformylation in supercritical carbon dioxide, U. S. Patent 4,437,938 (1984).

[26] R.P. DeFilippi, Separation of neutrals from tall oil soaps, U. S. Patent 4,349,415 (1982).

[27] J.G. Victor, Apparatus to concentrate and purify alcohol, U. S. Patent 4,508,928 (1985).

[28] K.D. Wagner, K. Brudi, N. Dahmen, H. Schmieder, Partition coefficient of organic substances in two-phase mixtures of water and carbon dioxide at pressures from 8 to 30 MPa and at temperatures 313 to 333 K. Part II, J. Supercrit. Fluids 15 (1999) 109 – 116.

[29] J.W. Tester, M. Modell, Thermodynamics and Its Applications, 3rd edition, Prentice Hall PTR.

[30] I.Kikic, Thermodynamic Properties – Phase Equilibria, Life Long Intensive Course, Supercritical Fluids – Green Solvents in Chemical Engineering (SCF – GSCE), 2009.

[31] M.J. Kamlet, R.M. Doherty, M.H. Abraham, Y. Marcus, R.W. Taft, Linear solvation energy relationship. 46. An improved equation for correlation and prediction of octanol/water partition coefficients of organic nonelectrolytes (including strong hydrogen bond donor solutes), J. Phys. Chem. 92 (1988) 5244.

[32] T. Wang, X.Y. Wang, R.L. Smith, Modeling of diffusivities in supercritical carbon dioxide using a linear solvation energy relationship, J. Supercrit. Fluids 35 (2005) 18 – 25.

[33] F. Lagalante, T.J. Bruno, Modeling the water-supercritical CO_2 partition coefficients of organics solutes using a linear solvation energy relationship, J. Phys. Chem. B 102 (1998) 907.

[34] L.P. McMaster, Macromolecules 6, 760 (1973)

[35] O. Redlich, J.N.S. Kwong, Chem.rev. 44 (1949) 233.

[36] G.Soave, Chem. Eng. Science 27 (1972) 1197.

[37] G.M. Schneider, Phase equilibria of liquid and gaseous mixtures at high pressures. In Experimental Thermodynamics; Le Neindre, B., Vodar, B., Eds.; Butterworth: London, 2 (1975) 787−801.

[38] U. K. Deiters, G. M. Schneider, High pressure phase equilibria: experimental methods, Fluid Phase Equilibria, 29 (1986) 145-160.

[39] R. E. Fornari, P. Alessi, I. Kikic, High pressure fluid phase equilibria: experimental methods and systems investigated (1978–1987), Fluid Phase Equilibria, 57 (1990) 1 – 33.

[40] R. Dohrn, G. Brunner, High-pressure fluid-phase equilibria: Experimental methods and systems investigated (1988–1993), Fluid Phase Equilibria, 106 (1995) 213 – 282.

[41]A.M. Kartal , C. Erkey, Surface modification of silica aerogels by hexamethyldisilazane–carbon dioxide mixtures and their phase behavior, J. Supercrit. Fluids 53(2010), Pages 115 – 120.

[42] C. Secuianu, V. Feroiu, D. Geana. Phase behaviour for carbon dioxide + ethanol system: Experimental measurement and modeling with a cubic equation of state, J. Supercrit. Fluids 47 (2008) 109.

[43] S.N. Joung, C.W. Yoo, H.Y. Shin, S.Y. Kim, K.-P. Yoo, C.S. Lee, W.S. Huh, Measurements and correlation of high-pressure VLE of binary CO_2– alcohol systems (methanol, ethanol, 2-methoxyethanol and 2-ethoxyethanol), Fluid Phase Equilibria 185 (2001) 219 – 230.

[44] L.A. Galicia-Luna, A. Ortega-Rodriguez, D. Richon, New apparatus for the fast determination of high-pressure vapor– liquid equilibria of mixtures and of accurate critical pressures, J. Chem. Eng. Data 45 (2000) 265 – 271.

[45] D.Y. Peng, D.B. Robinson, A new two-constant equation of state, Ind. Eng. Chem. Fundamen. 15 (1976) 59 – 64

[46] S.I. Sandler, Chemical and Engineering Thermodynamics, third edition, John Wiley & Sons, Inc., 1999.

[47] C.L. Yaws Handbook of Thermodynamic Diagrams, Gulf Pub. Co., Houston, 1996.

[48] W.E. Acree, Thermodynamic properties of nonelectrolyte solutions, Academic Press, New York, 1984.

[49] J. Zielkiewicz, (Vapour + liquid) equilibrium in (N,N-dimethylactemide + methanol + water) at the temperature of 313.15 K, J. Chem. Thermodynamics 35 (2003) 1993 – 2001.

[50] A. Bamberger, G. Sieder, G. Maurer, High pressure phase equilibrium of the ternary system carbon dioxide + water + acetic acid at temperatures from 313 to 353 K, J. Supercrit. Fluids 32 (2004) 15 – 25.

[51] J.M.Smith, H.C. Van Ness, M.M. Abbott, Introduction to Chemical Engineering Thermodynamics, seventh edition, McGraw-Hill, 2005.